



Universidad Autónoma
de Madrid

Biblos-e Archivo
Repositorio Institucional UAM

Repositorio Institucional de la Universidad Autónoma de Madrid

<https://repositorio.uam.es>

Esta es la **versión de autor** del artículo publicado en:

This is an **author produced version** of a paper published in:

European Journal of Medicinal Chemistry 157.5 (2018): 294-309

DOI: <https://doi.org/10.1016/j.ejmech.2018.07.030>

Copyright: © 2018 Elsevier Masson SAS.

This manuscript version is made available under the CC-BY- NC-ND 4.0 licence

<http://creativecommons.org/licenses/by-nc-nd/4.0/>

El acceso a la versión del editor puede requerir la suscripción del recurso

Access to the published version may require subscription

Design and synthesis of multipotent 3-aminomethylindoles and 7-azaindoles with enhanced protein phosphatase 2A-activating profile and neuroprotection

Rocío Lajarín Cuesta ^a, Raquel L. Arribas ^a, Carmen Nanclares ^a, Eva M. García-Frutos ^b, Luis Gandía ^a, and Cristóbal de los Ríos ^{a,c,*}

^a Instituto-Fundación Teófilo Hernando and Departamento de Farmacología y Terapéutica, Universidad Autónoma de Madrid, C/ Arzobispo Morcillo, 4, 28029 Madrid, Spain

^b Instituto de Ciencia de Materiales de Madrid, Consejo Superior de Investigaciones Científicas, C/ Sor Juan Inés de la Cruz, s/n, 28049, Madrid, Spain

^c Instituto de Investigación Sanitaria, Hospital Universitario de la Princesa, C/ Diego de León, 62, 28006, Madrid, Spain

Corresponding author: Cristóbal de los Ríos, e-mail address:

cristobal.delosrios@inv.uam.es

Abbreviations: A β , amyloid beta peptides; AD, Alzheimer's disease; I_{Ca}, Ca²⁺ currents; NFT, neurofibrillary tangles; NMDA, *N*-methyl-D-aspartate; OA, okadaic acid; PAD, PP2A-activating drugs; PD, Parkinson's disease, pNPP, *p*-nitrophenol phosphate; PP2A, phosphoprotein phosphatase 2A; *p*Tau, phosphoTau; PSA, polar surface area; R/O, rotenone plus oligomycin A; VGCC, voltage-gated Ca²⁺ channels.

ABSTRACT

We report the synthesis and pharmacological evaluation of new 3-aminomethylindoles derivatives with neuroprotective properties designed to present multi-target activity centered on reducing the neuronal Ca^{2+} overload and preventing phosphatase 2A (PP2A) inhibition, which are two important early physiopathological events observed in neurodegenerative scenarios. Chemical syntheses of proposed compounds were achieved in two straightforward reaction steps with high yields. Most of the compounds mitigated the okadaic acid-provoked inhibition of PP2A and protected SH-SY5Y cells against toxic stimuli related to Tau-hyperphosphorylation and oxidative stress, similarly to the observed in Alzheimer's disease (AD). In addition, some of them mitigated the Ca^{2+} overload induced by depolarization. The derivative 1-(1-benzyl-5-chloro-1*H*-indol-3-yl)-*N,N*-dimethylmethanamine (**19**) outstood by its high recovery of the PP2A activity and blockade of voltage-gated Ca^{2+} channels, accompanied by good neuroprotective profile. These findings make this compound eligible for further preclinical assays with the goal of positioning new innovative drugs for the treatment of AD.

Keywords: Gramine, multi-target strategy, PP2A, Ca^{2+} channels, neuroprotection, Alzheimer's disease

1. Introduction

Indole alkaloids are considered as one of the most successful small molecule drugs. Both traditional medicine and current marketed drugs are full of examples where the indole constitutes a chief part of the chemical structure, being the 5% of the total FDA-approved drugs. Interestingly, two third of them present a 3-aminoethylindole moiety, which is indeed found in paradigmatic drugs families such as the ergot alkaloids (ergotamine, cabergoline, nicergoline, ergometrine, etc), the triptans (sumatriptan, zolmitriptan, almotriptan, rizatriptan, etc), reserpine and related vinca alkaloids (deserpidine, rescinnamine, yohimbine, etc) or the blockbuster tadalafil. In addition, endogenous substances such as tryptophan, 5-HT or melatonin are also 3-aminoethylindoles (Fig. 1).

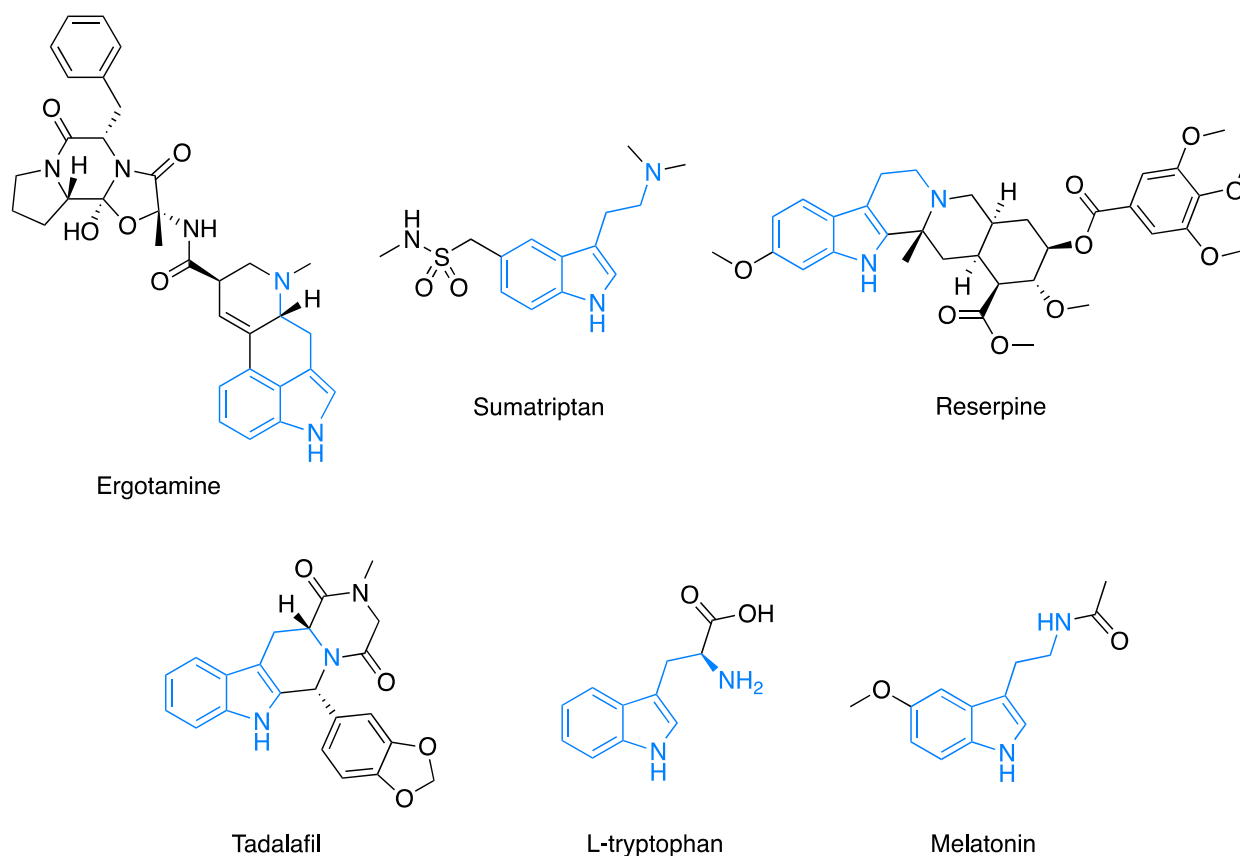


Fig. 1. Highlighted examples of FDA-approved natural products, synthetic drugs, and endogenous indoles. All of these examples possess the 3-aminoethyl substructure, traced in blue. **(PLEASE USE COLOR FOR THIS FIGURE)**

Conversely, much less interest, but not negligible, has aroused the therapeutic use of their homologous 3-aminomethylindoles [1-5]. Among all the indole-based FDA-approved drugs, such moiety can only be appreciated in the highly complex vinorelbine (Fig. 2). Gramine (**1**, Fig. 2), extracted from the family plant of the Poaceae, is the simplest example of 3-aminomethylindole discovered in biota [6]. Gramine has been object of several pharmacological studies, highlighting some of effect on the serotonergic system [7] or on mitochondrial bioenergetic [8]. Synthetic analogues of **1** have shown pharmacological activities such as antioxidant and anti-inflammatory [9, 10], anti-serotonergic [11] or cell Ca^{2+} modulators [12]. Moreover, **1** and its analogues have been used as precursors for the synthesis of a huge amount of indole derivatives, taking advantage their easy transformation through a retro-Mannich type reaction in acidic media into intermediates susceptible to smoothly suffer nucleophilic substitutions [13]. However, this chemical reactivity has hindered their positioning as investigational drugs. In this context, our research group has humbly contributed to set up experimental conditions that improve chemical stability and handling of **1** derivatives [14], facilitating their isolation and biological assessment. As a result, we have recently reported several **1** derivatives with interesting neuroprotective properties related to a dual pharmacological profile, the mitigation of neuronal Ca^{2+} overload and the reactivation of the Ser/Thr phosphatases enzymatic activity, among which the derivative ITH12657 (**2**) (Fig. 2) outstood by its wide-spectrum neuroprotective actions [14, 15].

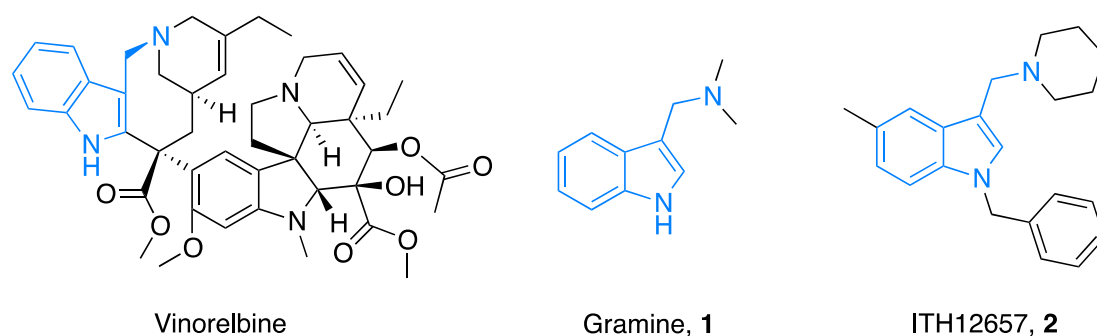


Fig. 2. Selected examples of 3-aminomethylindoles. Vinorelbine, the only drug in clinic possessing this moiety; gramine (**1**), as the simplest natural product, and its synthetic derivative ITH12657 (**2**) [14], under investigation for central nervous system diseases. **(PLEASE USE COLOR FOR THIS FIGURE)**

This multipotent feature makes these compounds of interest for the treatment of several human diseases where the alteration of both cell Ca^{2+} homeostasis and protein phosphorylation occur. Among them, neurodegenerative diseases like Alzheimer's (AD) prevail, due to the social and economic issues that entail, exacerbated by the lack of efficient medicines to face them [16]. In the case of AD, the alteration of cytosolic Ca^{2+} levels evidenced in vulnerable neurons is a widely observed characteristic [17, 18]. In this context, it is worthwhile mentioning that memantine, which diminishes the Ca^{2+} influx through the *N*-methyl-D-aspartate-sensitive glutamate (NMDA) receptors [19], is one of the few prescribed drugs for AD, along three anticholinesterasics (galantamine, donepezil, and rivastigmine) [20].

On the other hand, hyperphosphorylation of Tau protein that drives to the formation of the so-called neurofibrillary tangles (NFT) is one of the most validated therapeutic

targets in AD [21]. Although the real causes behind the AD onset remain elusive, increasing evidences reveal that, after the senile plaques formation by aggregation of amyloid β ($A\beta$) peptides, the generation of NFT, formed by hyperphosphorylated Tau proteins, is an essential event for the progression of the disease [22], in such a way that the sole presence of senile plaques accompanied by a total absence of NFT is characteristic of aged patients without dementia symptoms [23, 24].

Otherwise, therapeutic approaches to treat AD, such as those targeting amyloidogenesis, the use of pro-cholinergic drugs, or several antioxidant-based strategies, have failed [25, 26]. Not even drugs capable of inhibiting Tau kinases have afforded the expected crops [27]. In this sense, the activation of the opposite process, namely Tau dephosphorylation, mostly performed by the Ser/Thr phosphatase PP2A [28], has raised marginal interest in drug discovery [29], despite there is a plethora of biomedical literature reporting that PP2A enzymatic activity is key for the correct phosphorylation state of Tau [30], and more, PP2A down-regulation has been observed in neurodegenerative diseases like AD [31], Parkinson's disease (PD) [32], and amyotrophic lateral sclerosis [33], among others [34].

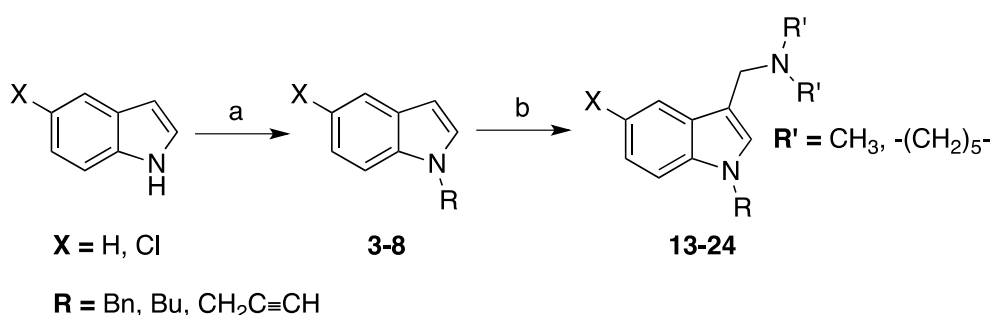
By these reasons, a multi-target strategy based on activating Tau dephosphorylation and mitigating neuronal Ca^{2+} overload keeps being an interesting therapeutic alternative for the development of innovative potential drugs for AD. Attempting to optimize the neuroprotective properties of the lead compound **2**, we herein describe the design, synthesis, and pharmacological assessment of gramine derivatives that present different substitution at C5, as well as aza-indole analogues, assessing the effect of these chemical modifications on both PP2A-activating potential and blockade of voltage-gated Ca^{2+} channels (VGCC).

2. Results and Discussion

2.1. Chemistry

The design of new **1** analogues aimed at enhancing their activity as PP2A-activating drugs (PAD) [35] to favor the dephosphorylation of NFT-aggregating Tau proteins, while maintaining VGCC blocking properties. With this purpose, we selected as substituents at the indole nitrogen those present in the best PAD of the previous family of **1** derivatives, i.e. benzyl, *n*-butyl, and propargyl. Modifications at C5 of the indole ring aimed to replace the metabolism-sensitive methyl group present in **2** (Fig. 2) by a more stable group or by its removal. Thus, the isosteric replacement of the methyl group by a chlorine atom was one of the chemical strategies selected, in order to improve the metabolic stability without losing biological activity. In addition, the relevance of substitution at C5 for the pharmacological properties studied was challenged with the preparation and further evaluation of non-substituted analogues **13–18**. Another remarkable modification was replacing the benzene-fused ring by a pyridine, to access the corresponding 7-azaindole analogues (formally pyrrolo[2,3-*b*]pyridines). We selected the easily accessible 5-bromo and 5-methoxy substitutions to start probing these new aza-indoles. The designed ligands are supposed to present more druggable properties, according to computational prediction centered on parameters of drug-likeness (Table S1, supplementary material). Such computational prediction included the Lipinsky's rule of 5 (molecular weight, clog P, and number of hydrogen bonds donors and acceptors) [36], the polar surface area (PSA), and, since the proposed derivatives possess ionizable groups, both pK_a (of the most basic center) and clog D [37] (Table S1, supplementary material). Most of

the compounds fulfilled the requirements for druggability, except compound **20** [$X = \text{Cl}$, $R = \text{Bn}$, $R' = -(\text{CH}_2)_5-$, Scheme 1] that showed two alerts (Table S1, supplementary material). However, realizing that it could be considered as the closest isoster of the lead compound **2**, it was synthesized and biologically assessed, too. With regard to the 7-azaindole derivatives, they drew a significant decrease in both clog P and clog D, except for compound **26**, which showed a slight alert in clog D (Table S1, supplementary material).



Scheme 1. Preparation of **1** derivatives. Reagents and conditions: (a) (1) NaH, DMSO, rt, 1–2 h, (2) alkyl or benzyl halide, rt, 1–2 h; (b) Me_2NH (aq) or piperidine, HCHO (aq), AcOH, 0 °C to rt, 2–5 h.

Compounds were prepared in two steps, starting with a *N*-alkylation reaction. 1*H*-indoles were deprotonated with NaH at room temperature, for 1 h in the case of the chlorinated substrate, and 2 h in the case of non-substituted 1*H*-indole. Afterwards, the corresponding alkyl or benzyl halide was added, to furnish intermediates **3–8** in excellent yields (Scheme 1), without further chromatographic purification. Despite this reaction classically recruits DMF as solvent [1, 38], we alternatively use DMSO [39, 40] because of its easier removal after the work-up. For the *N*-alkylation of 7-

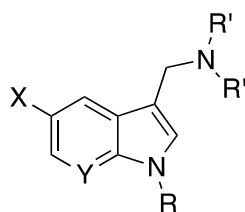
amine, either dimethylamine or piperidine are first mixed in AcOH and then the resulting solution injected to the reaction mixtures. This is presumably one of the causes of the scattered reactions yields found in literature for the synthesis of *N,N*-dimethylaminomethyl-3-indoles and related analogues. The other, in our opinion, is that some authors conduct Mannich reaction over *N1*-unsubstituted indoles for then to promote the *N*-alkylation [1]. Otherwise, taking into account that such *N*-alkylation confers stability *versus* the possible retro-Mannich reaction of 3-aminomethyl-1*H*-indoles, we consider a better election to promote Mannich reaction over *N*-alkylated indoles. Few examples in literature report the use of ZnCl₂ in ethanol instead acetic acid to promote Mannich reaction in similar indoles, but describing lower yields and longer reaction times than those shown herein [43]. As mentioned before, 3-aminomethyl-1*H*-indoles suffer a retro-Mannich process leading to the generation of 3-methylen-3*H*-indoles in acidic aqueous. To avoid such by-reaction, work-ups were carried out at pH > 10 (NaOH), chlorinated solvents were neutralized from acid traces with basic alumina, and flash chromatography, when necessary, was executed with basic alumina as stationary phase. Due to most of the compounds appear as oils of complicated manipulation and limited aqueous solubility, they were salinized to their oxalate salts, thus becoming white powdered solids, highly soluble (10 mM) in aqueous buffers, possessing high chemical stability, confirmed by ¹H-NMR length dissolved in D₂O. In contrast, ¹³C-NMR spectra of oxalates were carried out using DMSO-*d*₆, to get sufficient concentration for adequate acquisition (Supplementary material).

2.2. Gramine (1) derivatives mitigated the okadaic acid-induced Ser/Thr phosphatases inhibition

The rationale behind the development of the **1** derivatives we pursue is that, by interacting with the catalytic subunit C of PP2A in a binding site that does not compromise the PP2A-leaded Tau-dephosphorylating enzymatic activity, compounds could avoid the approach of specific inhibitors to PP2A catalytic center, and at this way keep or recover the PP2A phosphatase activity, which is found out depressed in several neurodegeneration scenarios [28], such as that observed in AD, where it has been described high cytosolic levels of PP2A endogenous inhibitors. To probe this hypothesis, the PP2A inhibition is modeled by subjecting SH-SY5Y neuroblastoma cells to okadaic acid (OA), a marine toxin widely used as experimental model of Tau hyperphosphorylation [44]. Exposure to OA reproduces morphological and cognitive hallmarks of AD in both neuronal cultures and animal models as a consequence of the impairment of PP2A [45]. To monitor changes in the phosphatase activity of SH-SY5Y cell cultures, we selected the colorimetric method of the *p*-nitrophenol phosphate (pNPP).[46] Colorless pNPP is a chromogenic substrate of phosphatase enzymes that hydrolyze it to form yellow-colored *p*-nitrophenolate ($\lambda_{\text{abs}} = 405 \text{ nM}$). The NMDA receptor blocker memantine at 10 nM was used as reference compound in these experiments by its activating effect of PP2A [14].

Table 1

%Recovery of the okadaic acid (OA)-challenged Ser/Thr phosphatase activity of SH-SY5Y neuroblastoma cells in presence of compounds **13–32**.^a



Compound	Y	X	R	R'	%Recovery of PP2A activity
Memantine	-	-	-	-	28 ± 3*
13	CH	H	Bn	CH ₃	45 ± 9**
14	CH	H	Bn	-(CH ₂)-	37 ± 4**
15	CH	H	<i>n</i> Bu	CH ₃	12 ± 13 ^{ns}
16	CH	H	<i>n</i> Bu	-(CH ₂)-	30 ± 9*
17	CH	H	CH ₂ C≡CH	CH ₃	59 ± 12**
18	CH	H	CH ₂ C≡CH	-(CH ₂)-	17 ± 11 ^{ns}
19	CH	Cl	Bn	CH ₃	78 ± 11***
20	CH	Cl	Bn	-(CH ₂)-	27 ± 11 ^{ns}
21	CH	Cl	<i>n</i> Bu	CH ₃	39 ± 13*
22	CH	Cl	<i>n</i> Bu	-(CH ₂)-	38 ± 15*
23	CH	Cl	CH ₂ C≡CH	CH ₃	23 ± 6*
24	CH	Cl	CH ₂ C≡CH	-(CH ₂)-	44 ± 13**
25	N	Br	Bn	CH ₃	21 ± 10 ^{ns}
26	N	Br	Bn	-(CH ₂)-	31 ± 8**
27	N	Br	<i>n</i> Bu	CH ₃	34 ± 9*
28	N	Br	<i>n</i> Bu	-(CH ₂)-	22 ± 10 ^{ns}
29	N	Br	CH ₂ C≡CH	CH ₃	17 ± 5 ^{ns}
30	N	Br	CH ₂ C≡CH	-(CH ₂)-	25 ± 11 ^{ns}
31	N	OCH ₃	Bn	CH ₃	33 ± 7**

^aSH-SY5Y cells, previously preincubated with test compounds at 0.1 μM for 24 h, were treated with the selective PP2A inhibitor OA at 15 nM and compounds for 18 h more. Phosphatase activity was assessed by the *p*NPP colorimetric method. Data are mean of five assays ± SEM in triplicates, expressed as recovered phosphatase activity. ****p* < 0.001, ***p* < 0.01, **p* < 0.05, ns = not significant, respect to SH-SY5Y neuroblastoma cells exposed to OA in absence of compounds.

Following the protocol described in the experimental section, SH-SY5Y cells subjected to OA 15 nM for 18 h suffered a decrease of 26 ± 2% in the phosphatase activity, without compromising cell viability (unlike the exposure to OA at 20 nM for 20 h, which decreased SH-SY5Y cells viability in a significant fashion, as shown in the neuroprotection experiments). Most of the compounds softened the drop of the phosphatase activity in OA-treated cells in a significant manner (Table 1), recovering it up to 78% result obtained when compound **19** was tested. Globally, this family of **1** derivatives diminished the effects of OA in a 34 ± 4%. Stressing on structure-activity relationships, benzyl-substituted **1** analogues recovered PP2A activity by an average of 40%, whilst those bearing butyl or propargyl groups did it by about a 30%. Similarly, a recovery average of 40% was also observed in those derivatives presenting chlorine or methoxy group at C5, which was much better than those observed in brominated or non-substituted analogues. The replacement of aromatic fused ring from benzene to pyridine to furnish derivatives **25–32** did not affected PAD activity dramatically, but an slight drop of the averaged %recovery was

appreciated. Similarly, the *N,N*-dimethylaminomethyl moiety at C3 afforded slightly better recovery than compounds bearing a piperidinylmethyl moiety at C3 analogues. Thus, the most sensible substitution seems to be that at the indole nitrogen. Collecting the best options for each chemical substitution proposed, a compound that presented benzyl at the indole nitrogen, chlorine or methoxy at C5, benzene as aromatic fused ring, and dimethylamine instead of piperidine, should theoretically be the best PP2A-activating compound. Indeed, compound **19** (R = Bn; R' = Me; X = Cl; Y = CH) presented the best %recovery of the PP2A enzymatic activity (75%, Table 1). Taking into account that OA is about 500-fold more selective for inhibiting PP2A than for PP1 [47], we firmly state that the reactivation of the phosphatase activity carried out by our compounds in presence of OA 15 nM (a concentration where PP1 is marginally affected) is directly ascribed to their ability to counteract the OA-induced PP2A inhibition. We have proved this hypothesis through western-blot analysis, testing the effect of the best PAD, i.e. **19**, in the phosphorylation rate of Tau (Fig. 3).

2.3. Compound **19** reduced phosphorylation of Tau of SH-SY5Y neuroblastoma cells exposed to OA

It is important to remark that PP2A is by far the principal phosphatase enzyme of Tau protein [28]. The quantification of phosphoTau (pTau) levels was achieved with the primary antibody anti-pTau AT8 that recognizes pSer 202 and pThr 205 phosphoepitopes, extensively found in NFT-forming Tau aggregates [48].



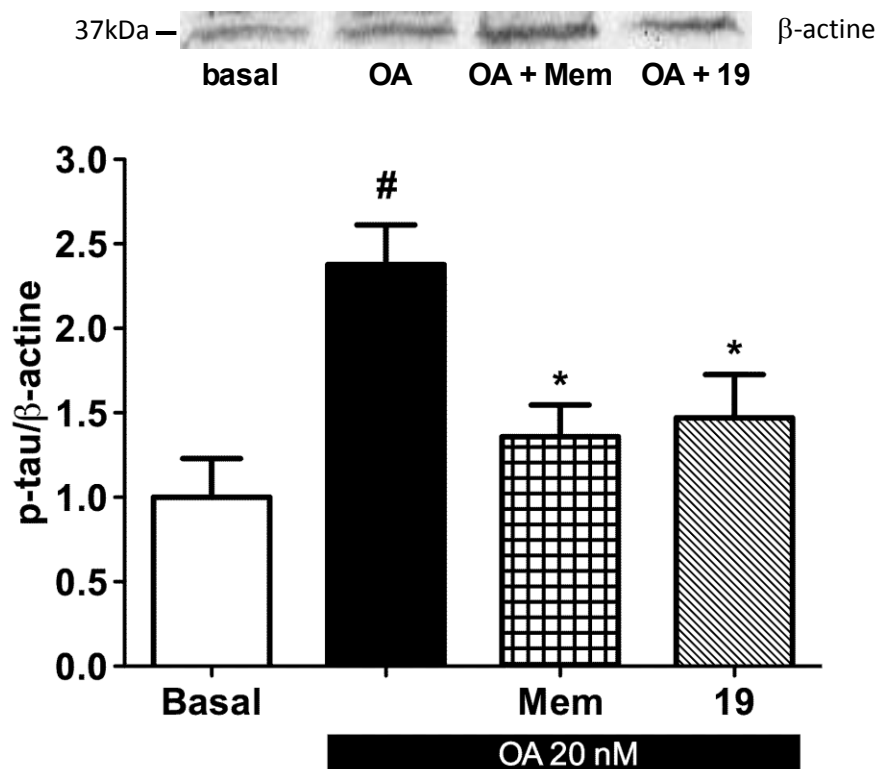


Figure 3. Effect of compound **19** on the 15 nM OA-induced Tau phosphorylation in SH-SY5Y neuroblastoma cells. Top, immunoblot of a representative experiment. Data are expressed as the mean \pm SEM of three independent experiments. # $p < 0.05$, compared with basal group, * $p < 0.05$ compared with cells subjected to OA in absence of compounds. Compound **19** was tested at the concentration of 100 nM. Memantine (Mem) 10 nM was used as a reference compound.

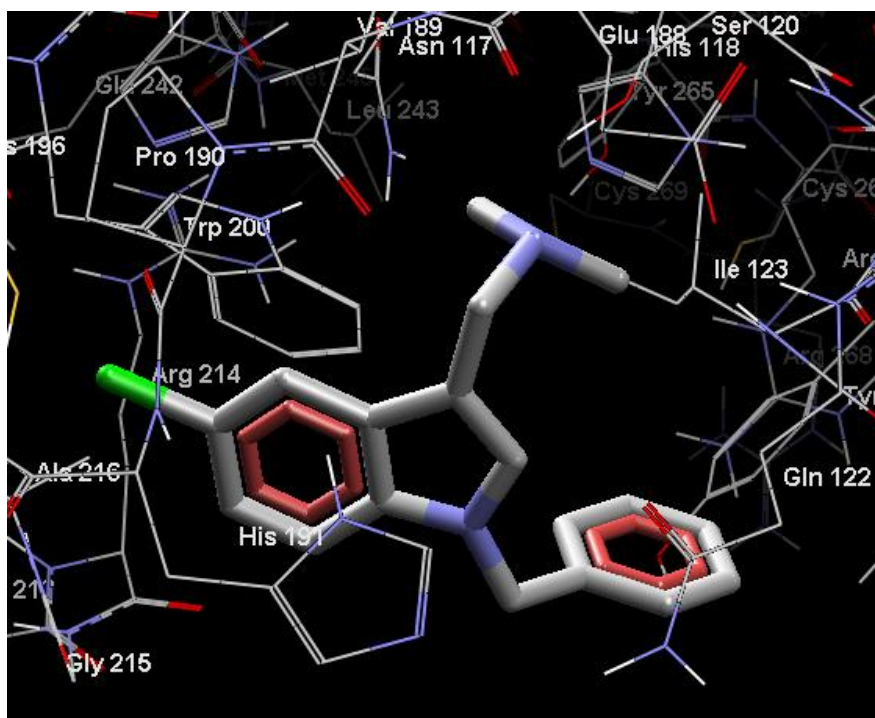
The 24 h-exposure of the selective PP2A inhibitor OA to SH-SY5Y neuroblastoma cells augmented almost 2.5-fold the phosphorylation rate of Tau at Ser 202 and Thr 205, which was noticeably prevented by the presence of **19** at 0.1 μ M (Fig. 3), the same concentration used for enzymatic assays shown in Table 1. Hence, we can

confirm that compound **19** avoids the inhibition of PP2A, which could drive, for instance, to the NFT-generating Tau hyperphosphorylation observed in AD. With the goal of finding structural clues for this highlighted pharmacological activity, molecular docking studies of **19** with PP2A were performed.

*2.4. Docking studies on the interaction of **1** derivatives and PP2A*

Molecular docking studies were implemented to figure the possible interactions of PP2A with **1** derivatives, using its 3D structure deposited in the Protein Data Bank (ID: 2IE4; www.rdcdb.org) [49]. We selected derivative **19** to run the docking experiments (Fig. 4), as it was the best PAD of the family, and compound **32** (Fig. 5), as the most active 7-azaindole **1** derivatives, which exerted a 47% recovery of PP2A enzymatic activity (Table 1).

(A)



(B)

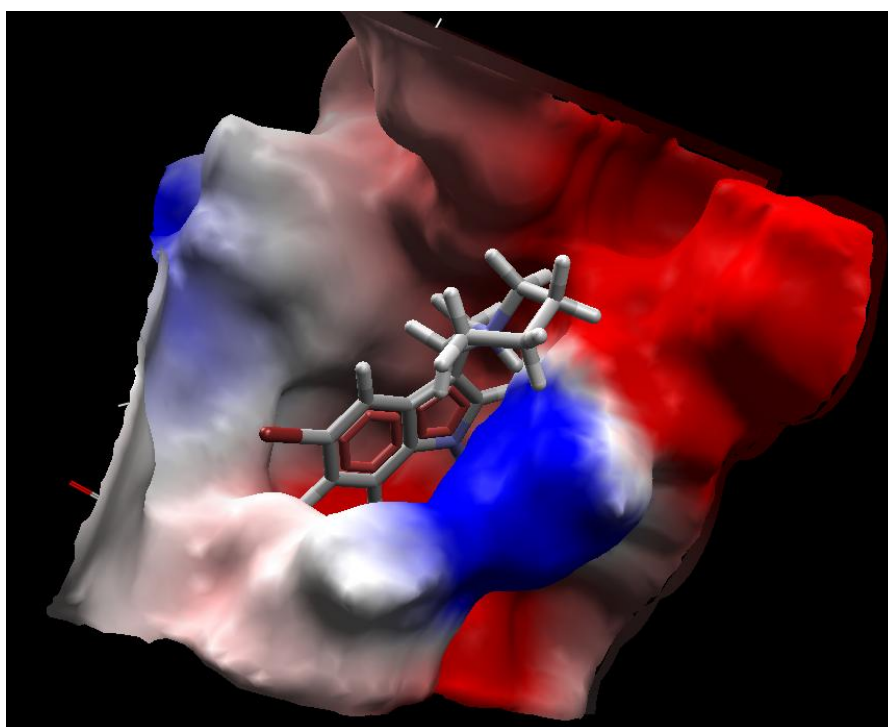


Fig. 4. Molecular docking of **19**—PP2A complex. (A) Pose of **19** with the interacting amino acid residues within a 6 Å radius. (B) Electrostatic map where the charge-transfer interaction between the indole ring of **19** and the positively-charged His 191

is observed (high electron density areas are red-colored, while electron-deficient areas are in blue). **(PLEASE USE COLOR FOR THIS FIGURE)**

Fig. 4A shows compound **19** in a shape able to establish a strong H-bond between its dimethylamine group, protonated at physiological pH, and the hydroxyl of Ser 120 ($d = 1.75 \text{ \AA}$). The benzene-fused ring of **19** seems to interact in planar (π - π) hydrophobic fashion with Trp 200, while the electron-filled indole-forming pyrrole finely faces the electron-demanding His 191 (Fig. 4B).

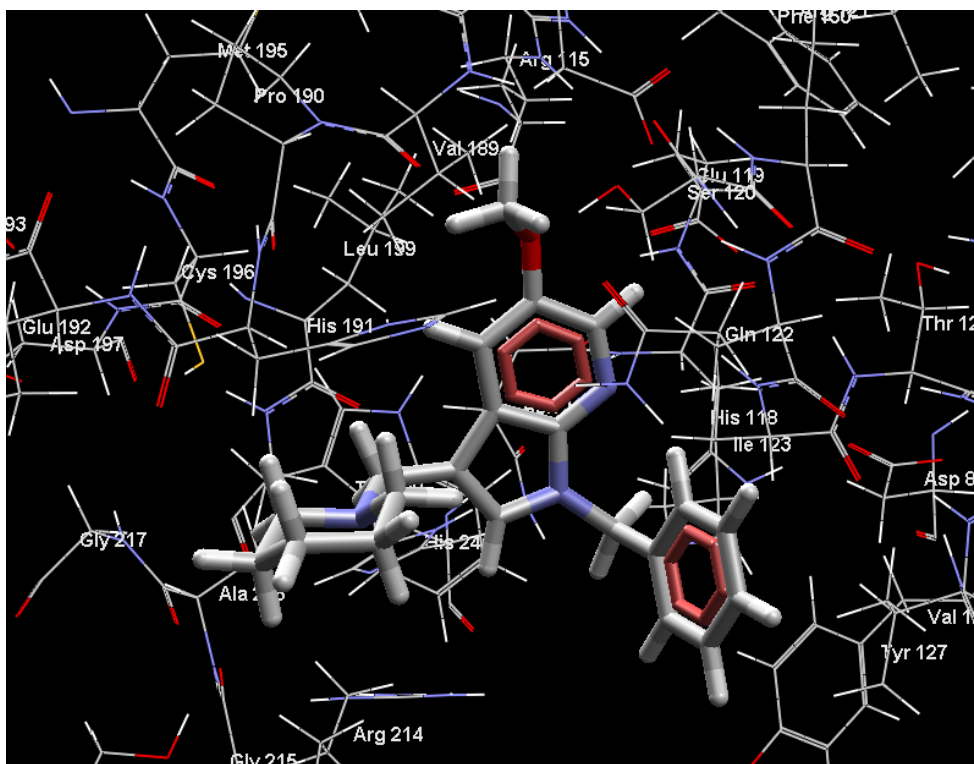


Fig. 5. Molecular docking of **32**—PP2A complex. Pose of **32** with the interacting amino acid residues within a 8 \AA radius. **(PLEASE USE COLOR FOR THIS FIGURE)**

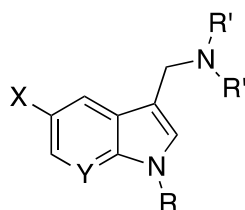
As far as the 7-azaindole analogue **32**, it can be appreciated a weak H-bond between Ser 120 and the methoxy group at C5, where the steric hindrance elicited by methyl would prevent a better fit. Otherwise, **32** nicely poses into the hydrophobic pocket defined by Ala 216 (to the piperidine substituent; $d = 3.59 \text{ \AA}$), Ile 123 and Val 126 (to the benzyl group; $d = 4.01$ and 3.86 \AA , respectively)(Fig. 5).

*2.5. Effect of **1** derivatives on the increases of neuronal Ca^{2+} stimulated by depolarization*

SH-SY5Y neuroblastoma is an excitable cell line that responds to extracellular exposure to 70 mM K^+ opening VGCC, and thus taking up ungovernable large amounts of Ca^{2+} that trigger neuronal death phenomena, resembling the Ca^{2+} overload evidenced in several neurodegenerative diseases such as AD [50]. Since several **1** derivatives described in literature behaved as Ca^{2+} -antagonists, we wondered whether these newly synthesized **1** derivatives related to head compound **2** could buffer depolarization-induced Ca^{2+} elevations, too. To respond this question, 96-well-plated SH-SY5Y cells were charged with the Ca^{2+} -sensitive fluorescent dye fluo-4, which detects cytosolic Ca^{2+} and its oscillation, and stimulated with an extracellular solution of 70 mM K^+ in presence of the test compounds. The well-known Ca^{2+} -antagonist nifedipine [51], was used in our experiments as reference compound. As shown in **Table 2**, Similarly, some **1** derivatives reduced the K^+ -stimulated Ca^{2+} increase through VGCC in SH-SY5Y cells monitored by fluo-4 (Table 2).

Table 2

Blockade of the high K⁺-Induced Ca²⁺ uptake by compounds **13–32** in SH-SY5Y neuroblastoma cells.^a



Compound	Y	X	R	R'	%blockade
Nifedipine	-	-	-	-	40 ± 5 ^{***}
13	CH	H	Bn	CH ₃	22 ± 6 [*]
14	CH	H	Bn	-(CH ₂)-	11 ± 7 ^{ns}
15	CH	H	<i>n</i> Bu	CH ₃	7 ± 5 ^{ns}
16	CH	H	<i>n</i> Bu	-(CH ₂)-	13 ± 8 ^{ns}
17	CH	H	CH ₂ C≡CH	CH ₃	3 ± 4 ^{ns}
18	CH	H	CH ₂ C≡CH	-(CH ₂)-	35 ± 5 ^{**}
19	CH	Cl	Bn	CH ₃	40 ± 6 ^{***}
20	CH	Cl	Bn	-(CH ₂)-	37 ± 7 ^{***}
21	CH	Cl	<i>n</i> Bu	CH ₃	23 ± 7 [*]
22	CH	Cl	<i>n</i> Bu	-(CH ₂)-	24 ± 8 [*]
23	CH	Cl	CH ₂ C≡CH	CH ₃	18 ± 11 ^{ns}
24	CH	Cl	CH ₂ C≡CH	-(CH ₂)-	32 ± 8 ^{**}
25	N	Br	Bn	CH ₃	46 ± 6 ^{***}

26	N	Br	Bn	-(CH ₂)-	15 ± 6 ^{ns}
27	N	Br	<i>n</i> Bu	CH ₃	10 ± 6 ^{ns}
28	N	Br	<i>n</i> Bu	-(CH ₂)-	9 ± 4 ^{ns}
29	N	Br	CH ₂ C≡CH	CH ₃	11 ± 6 ^{ns}
30	N	Br	CH ₂ C≡CH	-(CH ₂)-	8 ± 5 ^{ns}
31	N	OCH ₃	Bn	CH ₃	10 ± 6 ^{ns}
32	N	OCH ₃	Bn	-(CH ₂)-	19 ± 8 ^{ns}

^aSH-SY5Y cells, previously preincubated with test compounds at 1 μM or nifedipine at 3 μM for 10 min, were stimulated with a high K⁺ solution to get a final concentration of 70 mM in the extracellular medium, monitoring the subsequent cytosolic Ca²⁺ elevation with the fluorescent dye fluo-4. Compounds diminished such increase by the percentage expressed in the table. Data are mean of five assays ± SEM in triplicates. ***p < 0.001, **p < 0.01, *p < 0.05, and ns = not significant, respect to SH-SY5Y neuroblastoma control cells exposed to 70 mM K⁺ in absence of tested compounds.

Only 8 of 20 compounds blocked the Ca²⁺ entry exacerbated by depolarization in SH-SY5Y cells in a statistically significant manner. Interestingly, the presence of a chlorine atom at C5 favor better VGCC blockade (Table 2), what is consistent with its nature as bioisoster of the methyl group, present in the head compound **2**, which showed important Ca²⁺ antagonist properties [14]. Besides, benzyl group outstands as a privileged substituent over butyl and propargyl at the indole nitrogen. Most of the 7-aza-analogues **25–32** did not block VGCC but, surprisingly, compound **25** appears as the best blocker of the current family, what underlines the complexity to

infer structure-activity relationships over some biological targets such as ionic channels. The best VGCC blockers **19** and **25** were further studied with electrophysiological experiments using a whole-cell patch-clamp configuration, to directly measure Ca^{2+} currents (I_{Ca}) through VGCC of bovine chromaffin cells.

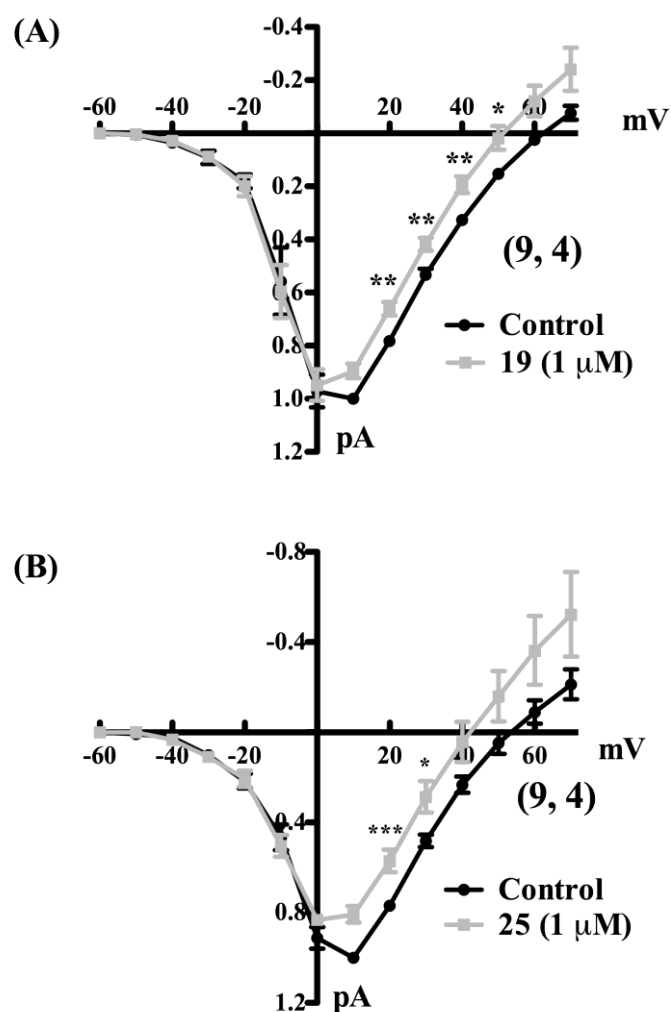


Fig. 6. Blockade of Ca^{2+} currents by **19** and **25** in bovine chromaffin cells.

Normalized intensity/voltage (I/V) relationship of I_{Ca} before (control, black line, A or B) and after treatment with compound 19 (grey line, A) or compound 25 (grey line,

B). Data are means \pm SEM of 9 cells from 4 cultures, as indicated in parentheses.

*** $p < 0.001$; ** $p < 0.01$; * $p < 0.05$, respect to control for each voltage.

To characterize blockade of I_{Ca} by **19** or **25**, we performed intensity vs voltage (I/V) curves, applying depolarizing pulses of 5×10^{-2} s from -60 to $+70$ mV each 20 s, in the presence or the absence of compounds. As shown in Fig. 6, both compounds produced a partial blockade of I_{Ca} that was statistically significant when positive depolarizing pulses were applied, without affecting the amplitude of I_{Ca} recorded at negative potentials. These data would indirectly suggest that the blocking effects of **19** and **25** on I_{Ca} are selective for non-L-type VGCC (i.e. N- or P/Q-type channels), as reported for **2** [14]. The absence of effects on L-type VGCC would elude cardiovascular-related side effects for these compounds.

Hence, five derivatives (**13**, **19**, **21**, **22**, and **24**) behaved as multipotent ligands, drawing a blockade of VGCC and maintaining the PP2A activity compromised by inhibitory actions. Among all the chemical modifications proposed, the substitution of chlorine at C5 and a benzyl group linked to the indole nitrogen would be maximizing this dual action. Hence, the pharmacological properties shown by **2** are matched by **24** and amenably improved by **19**, which indeed exerted a reduction of the pTau levels measured by western-blot (Fig. 3), although the use of other Tau antibodies would be necessary to confirm this attractive feature. In any case, further experiments were planned to assess whether this dual action achieved neuroprotection against toxic stimuli related to AD.

2.6. Neuroprotection experiments

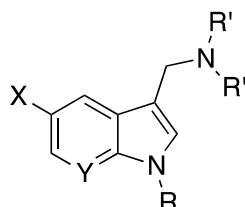
Before appraising the ability of compounds for counteracting toxic stimuli related to neurodegeneration in SH-SY5Y cells, we estimated their possible intrinsic toxicity in the same cell model, by *per se* exposing cell cultures to compounds for 48 h at much higher concentrations, up to 30 μ M, than those used for pharmacological activities and neuroprotection. Thus, none of the compounds reduced viability of SH-SY5Y cells measured by the 3-(4,5-dimethylthiazol-2-yl)-2,5-diphenyltetrazolium bromide (MTT) method at the concentration of 3 μ M, and most of them were harmless at 10 μ M (Fig. S1, supplementary material). Hence, the derivatives **13–32** would not damaging neurons at concentrations where they show PAD, Ca^{2+} -antagonist and neuroprotective activities.

According to the pharmacological activities of **13–32** shown in Table 1 and 2, we proposed to run the neuroprotective assays under two experimental models of neurodegeneration closely related to the progression of AD, i.e. Tau hyperphosphorylation and oxidative stress, monitoring the viability of SH-SY5Y cells in presence of compounds by the method of the MTT reduction [52]. Tau hyperphosphorylation-related damage was simulated by exposing SH-SY5Y cells to OA. Thus, when cells were subjected to the damage exerted by OA at 20 nM for 20 h, cell viability was reduced by $30 \pm 1\%$. In this situation, cells preincubated and coincubated with compounds **13–32**, relieved the OA-elicited loss of cell viability by the percentages expressed in Table 3, which was statistically significant for all compounds. Memantine at 10 nM was used as standard in these experiments for its protective actions against the impairment of PP2A enzymatic activity [14].

Table 3

% Protection^a by compounds **13–32** of the cell viability of SH-SY5Y neuroblastoma cells compromised by okadaic acid (OA)^b or the cocktail of rotenone plus oligomycin

A (R/O)^c



Compound	Y	X	R	R'	OA ^b	R/O ^c
Memantine	-	-	-	-	63 ± 2 ^{***}	-
Melatonin	-	-	-	-	-	36 ± 5 [*]
13	CH	H	Bn	CH ₃	67 ± 3 ^{***}	34 ± 3 ^{***}
14	CH	H	Bn	-(CH ₂)-	65 ± 4 ^{***}	28 ± 2 ^{***}
15	CH	H	<i>n</i> Bu	CH ₃	50 ± 3 ^{***}	20 ± 6 ^{ns}
16	CH	H	<i>n</i> Bu	-(CH ₂)-	55 ± 4 ^{***}	25 ± 5 ^{**}
17	CH	H	CH ₂ C≡CH	CH ₃	75 ± 2 ^{***}	32 ± 4 ^{***}
18	CH	H	CH ₂ C≡CH	-(CH ₂)-	58 ± 4 ^{***}	41 ± 3 ^{***}
19	CH	Cl	Bn	CH ₃	88 ± 2 ^{***}	32 ± 3 [*]
20	CH	Cl	Bn	-(CH ₂)-	62 ± 4 ^{***}	24 ± 2 ^{**}
21	CH	Cl	<i>n</i> Bu	CH ₃	93 ± 1 ^{***}	38 ± 3 [*]
22	CH	Cl	<i>n</i> Bu	-(CH ₂)-	98 ± 1 ^{***}	27 ± 5 [*]
23	CH	Cl	CH ₂ C≡CH	CH ₃	43 ± 6 ^{**}	26 ± 6 [*]
24	CH	Cl	CH ₂ C≡CH	-(CH ₂)-	55 ± 7 [*]	16 ± 2 ^{ns}
25	N	Br	Bn	CH ₃	84 ± 2 ^{***}	32 ± 4 [*]
26	N	Br	Bn	-(CH ₂)-	60 ± 4 ^{***}	25 ± 3 [*]

27	N	Br	<i>n</i> Bu	CH ₃	57 ± 4 ^{***}	18 ± 3 ^{ns}
28	N	Br	<i>n</i> Bu	-(CH ₂)-	98 ± 1 ^{***}	39 ± 3 [*]
29	N	Br	CH ₂ C≡CH	CH ₃	63 ± 5 ^{**}	17 ± 3 ^{ns}
30	N	Br	CH ₂ C≡CH	-(CH ₂)-	68 ± 3 ^{***}	13 ± 3 ^{ns}
31	N	OCH ₃	Bn	CH ₃	51 ± 5 ^{***}	29 ± 6 [*]
32	N	OCH ₃	Bn	-(CH ₂)-	62 ± 2 ^{***}	40 ± 6 ^{**}

^aData, assessed by the MTT method, are shown as the recovered %viability by compounds when the toxic stimulus is present. ^bSH-SY5Y cells preincubated with compounds at 0.1 μM for 24 h, and subjected to 20 nM OA and 0.1 μM of tested compounds for 20 h. ^cSH-SY5Y cells preincubated with compounds at 10 nM for 24 h, and subjected to R/O 30 and 10 μM in presence of compounds at 10 nM for 24 h more. Data are mean of five assays ± SEM by triplicates. ***p < 0.001, **p < 0.01, *p < 0.05, ns = not significant, respect to SH-SY5Y cells exposed to toxic stimulus in absence of compounds.

Establishing structure-activity relationships from neuroprotective experiments is always a tough challenge, due to neuroprotective compounds could dissipate neuronal damage through interactions with a plethora of proteins implicated in the physiopathological cascade triggered by the toxic stimulus. Indeed, when we analyzed the effect of compounds over the toxicity exerted by OA, no clear evidences of privileged substituents were found among all the synthetic alternatives proposed. Nevertheless, we appreciated that the propargyl group at the indole nitrogen (R = CH₂C≡CH) and both methoxy group and hydrogen at C5 (X = OCH₃, H) are the less efficacious chemical modifications to mitigate the OA-driven

neurotoxicity. In addition, there were five compounds able to recover the viability of OA-challenged SH-SY5Y cells by more than 80% (Table 3). Three of them (**19**, **21**, and **22**) modulated both PP2A-played phosphatase activity and cell Ca^{2+} overload (Table 1 and 2). These compounds are therefore merely considered multitarget-directed neuroprotectants.

Next, SH-SY5Y neuroblastoma cells were subjected to oxidative stress by administration of stressor cocktail formed by rotenone plus oligomycin A (R/O), which blocks complexes I and V of the mitochondrial electron transport chain, respectively, and therefore impairs ATP synthesis [53]. It is worthwhile mentioning that several models of oxidative stress related to aging produce PP2A inactivation [54], as well as neuronal Ca^{2+} dishomeostasis [55], where VGCC overactivation plays an essential role [56]. Thus, 24 h of exposure to the R/O cocktail at the concentration of 30 and 10 μM , respectively, diminished viability of SH-SY5Y neuroblastoma cells by $38 \pm 1\%$. Previously, we had observed that **1**, tested in a wide range of concentrations, featured a decent neuroprotective profile against R/O neurotoxicity from concentrations as low as 10 nM (data not shown), in a similar fashion to the well-known antioxidant and PP2A activator melatonin [57, 58]. This fact prompted us to test compounds **13–32** at 10 nM in the in vitro model of oxidative stress elicited by R/O in SH-SY5Y cells, although these compounds were actually not designed either to scavenge free radicals or bind any redox enzyme. Otherwise, 14 out 20 compounds healed part of the damage elicited by R/O (Table 3). None of the chemical substitutions outstood, but propargyl group at the indole nitrogen seems to be the less favored substituent to achieve neuroprotection. Compounds **18**, **21**, **28**, and **32** performed the best antioxidant effects, being better than the standard melatonin and reaching about 40% of protection (Table 3). Compound **19** also

deserves to be mentioned herein, as its 32% of protection against the R/O-evoked toxic signal, added to the best PAD profile (Table 1), the second best depolarization-stimulated Ca^{2+} blockade (Table 2), and its great neuroprotective effect against OA (88%, Table 3), make it the lead compound of the series. In addition, multipotent compounds **21** and **22** showed important neuroprotective actions, unlike **24**, which did not protect against the R/O toxicity, despite being PAD and VGCC blocker. Besides, the important Ca^{2+} antagonist effect of compound **25** (Fig. 6), though lacking PP2A up-regulatory actions, led to a decent neuroprotective profile in both models. On the other hand, the good neuroprotective profile of **28** (Table 3) opens the door to new experiments to figure out its real pharmacological mechanism of action, as it did not affect phosphatase activity or cell Ca^{2+} overload. As far as the 7-azaindole analogues **25–32**, they have not globally afforded better results than their benzene-fused analogues **13–24**. Otherwise, they would present beneficial physicochemical properties to feature acceptable pharmacokinetic parameters, such as the lower clog P, clogD_[7.4], pKa (Table S1, supplementary material) or minor in vitro toxicity (Figure S1, supplementary material). Finally, the family of chlorinated **1** derivatives evidenced the most promising biological activities. In our opinion, this should be due in part to the bio-isosteric nature of the chlorine atom as a first-election, metabolically stable, replacement for methyl groups, present in the head compound **2**. Its most promising derivative seems to be **19** that, although more western-blot analyses need to be executed to fully characterize its dephosphorylating effect on Tau, it herein demonstrated that reduces the levels of pTau measured by AT8 antibody, which recognizes phosphoepitopes at Ser 202 and Thr 205 sites.

3. Conclusions

In summary, we describe a family of optimized **1** derivatives designed to improve the PP2A-activating profile and, as a consequence, show a huge neuroprotective profile against the toxic stimulus elicited by the PP2A inhibitor OA. Thus, they can be considered PAD. According to the classification presented by Stock and co-workers [35], who claimed the existence of three types of PAD, which are 1) those inhibiting an inhibitory interaction, 2) those modulating enzymes responsible of post-translational modifications, and 3) those exerting an allosteric activation, our compounds would lay in the first postulation, as they hinder interactions of PP2A with selective inhibitors. These properties are accompanied with a noticeable protecting effect against the stressing consequences of a mitochondria-targeted oxidative stimulus, and capability to regulate neuronal Ca^{2+} . As a result, we have discovered several new **1** derivatives that behaved as multi-target drugs for two biological targets closely implicated in the AD progression. It is necessary to highlight that, although both targets are intrinsically interesting, their simultaneous intervention can offer not only additive effects, but also synergistic, as both are interconnected. For instance, PP2A modulates the kinetic of VGCC [59, 60]. Although there are no previously described compounds from other research groups designed to modulate these both pharmacological targets in a multi-target fashion, memantine could be considered the first example, as it controls neuronal Ca^{2+} by antagonizing NMDA receptors, and is able to prevent the inhibition of PP2A-controlled phosphatase activity [61]. Hence, memantine would be the most direct antecedent of our drug discovery program, and the fact that it is one of the few drugs approved for AD treatment would back the validation of our working hypothesis. The multi-target based drug design has unsuccessfully pursued an efficient cure for AD in the last

two decades [62, 63]. The classical multi-target strategies keep paying attention to design principally cholinergic drugs possessing an additional pharmacological activity [64-69]. Besides, there is an increasing interest in exploring other therapeutic alternatives, sustained by the discovery of new biological targets implicated in AD that possess a potential druggability, such as the search of microtubule-stabilizing agents [70] or drugs suppressing NMDA receptors active subunits [71]. As far as our multi-target approach, VGCC and PP2A are not new biological targets, but we consider they have not been sufficiently investigated for neurodegeneration, and much less under as part of a multi-target strategy. In addition, this therapeutic alternative could also have interest in other diseases such as PD [32, 72], cerebral ischemia [73], traumatic brain damage [74, 75] or pain [76, 77], as both Ca^{2+} homeostasis and PP2A are biological target compromised in these pathologies.

4. Experimental Section

4.1. General Procedures

5-Bromo-1*H*-pyrrolo[2,3-*b*]pyridine was purchased from fluorochem (Hadfield, UK). 5-Chloro-1*H*-indole, 1*H*-indole, gramine, memantine, melatonin, rotenone, and OA were purchased from Merck (Madrid, Spain). Oligomycin A was acquired in Santa Cruz Biotechnology (Dallas, TX). Solvents and general reagents for synthesis were acquired from VWR (Fountenai/Sous/Bois, France). Reactions were controlled by TLC of silica gel for the preparation of intermediates **3–12**, and of aluminum oxide for the preparation of compounds **13–32**, on TLC-PET foils (Sigma-Aldrich/Merck), detecting bands at 254 nm. Reactions were purged with vacuum/argon cycles and conducted under argon atmosphere. To purify products, automatized flash

chromatography (Biotage ISOLERA ONE, Uppsala, Sweden) were used when necessary, using pre-charged silica gel SNAP columns (Biotage) for intermediates **3–12**, or SNAP columns filled with basic aluminum oxide (Brockmann I; Sigma-Aldrich/Merck) for products **13–32**. Melting points of final compounds were obtained with an Stuart SMP-10 apparatus (Staffordshire, UK) and are uncorrected. ^1H and ^{13}C NMR spectra were performed in an AVANCE 300 MHz (Bruker) and expressed as parts per million (ppm). The tested compounds had a purity > 95%, confirmed by elemental analysis in a LECO CHNS-932 station (Analyses indicated by the symbols of the elements were within the 0.4% of the theoretical value).

4.2 General Method for the N-alkylation of 1H-indole or 5-chloro-1H-indole

According to the method described by Na and co-workers [78], with some modifications [14], NaH (1.2 equiv, 60%) was added to 5-chloro-1*H*-indole or 1*H*-indole (1 equiv) in DMSO (3.5–5 mL/mmol) under Ar at rt, and the mixture stirred for 1 h for 5-chloro-1*H*-indole or 2 h for 1*H*-indole. Then, the alkyl or benzyl halide (1.2–1.4 equiv) was injected and the reaction stirred for 2–4.5 h, monitoring the evolution of the reaction by TLC. When this was completed, water (10 mL/mmol) was added and the mixture extracted with CH_2Cl_2 (3 × 30 mL/mmol), dried with Na_2SO_4 (anh.), filtered, and concentrated, obtaining pure compounds without further purification.

4.3. 1-benzyl-1H-indole (3)

According to the General Method for the *N*-alkylation of 1*H*-indole or 5-chloro-1*H*-indole, 1*H*-indole (250 mg, 2.13 mmol) [DMSO (8 mL), NaH (102 mg, 2.56 mmol),

benzyl bromide (303 μ L, 2.56 mmol)] yielded **3** (438 mg, > 99%) with spectral data according to literature [79].

4.4. 1-butyl-1H-indole (**4**)

According to the General Method for the *N*-alkylation of 1*H*-indole or 5-chloro-1*H*-indole, 1*H*-indole (250 mg, 2.13 mmol) [DMSO (8 mL), NaH (102 mg, 2.56 mmol), 1-iodobutane (291 μ L, 2.56 mmol)] yielded **4** (339 mg, 92%) with spectral data according to literature [80].

4.5. 1-(prop-2-yn-1-yl)-1H-indole (**5**)

According to the General Method for the *N*-alkylation of 1*H*-indole or 5-chloro-1*H*-indole, 1*H*-indole (250 mg, 2.13 mmol) [DMSO (8 mL), NaH (102 mg, 2.56 mmol), 3-bromoprop-1-yne (285 μ L, 2.56 mmol)] yielded **5** (289 mg, 87%) with spectral data according to literature [81].

4.6. 1-benzyl-5-chloro-1H-indole (**6**)

According to the General Method for the *N*-alkylation of 1*H*-indole or 5-chloro-1*H*-indole, 5-chloro-1*H*-indole (294 mg, 1.94 mmol) [DMSO (9 mL), NaH (93 mg, 2.33 mmol), benzyl bromide (275 μ L, 2.33 mmol)] yielded **6** (434 mg, 93%) with spectral data according to literature [82].

4.7. 1-butyl-5-chloro-1H-indole (**7**)

According to the General Method for the *N*-alkylation of 1*H*-indole or 5-chloro-1*H*-indole, 5-chloro-1*H*-indole (294 mg, 1.94 mmol) [DMSO (9 mL), NaH (93 mg, 2.34 mmol), 1-iodobutane (265 μ L, 2.33 mmol)] yielded **7** (384 mg, 95%). ^1H NMR (300 MHz, acetone- d_6) δ 7.61 (bd, 1H, J = 2.1 Hz, H4), 7.38 (bd, 1H, J = 8.7, H7), 7.27 (d, 1H, J = 3.3 Hz, H2), 7.16 (dd, 1H, J = 2.1, 8.7 Hz, H6), 6.45 (dd, 1H, J = 0.9, 3.3 Hz, H3), 4.11 (t, 2H, J = 7.2 Hz, NCH₂), 1.81–1.69 (m, 2H, NCH₂CH₂), 1.35–1.20 (m, 2H, CH₂CH₃), 0.90 (t, 3H, J = 7.2 Hz, CH₃).

4.8. 1-(prop-2-yn-1-yl)-5-chloro-1H-indole (**8**)

According to the General Method for the *N*-alkylation of 1*H*-indole or 5-chloro-1*H*-indole, 5-chloro-1*H*-indole (245 mg, 1.62 mmol) [DMSO (8 mL), NaH (78 mg, 1.94 mmol), 3-bromoprop-1-yne (252 μ L, 2.26 mmol)] yielded **8** (300 mg, 98%). ^1H NMR (300 MHz, acetone- d_6) δ 7.63 (d, 1H, J = 2.1 Hz, H4), 7.50 (bd, 1H, J = 8.7, H7), 7.40 (d, 1H, J = 3.0 Hz, H2), 7.21 (dd, 1H, J = 2.1, 8.7 Hz, H6), 6.50 (dd, 1H, J = 0.9, 3.0 Hz, H3), 5.03 (d, 2H, J = 2.7 Hz, CH₂), 2.95 (t, 1H, J = 2.7 Hz, CH).

4.9. General Method for the N1-alkylation of 1H-pyrrolo[2,3-*b*]pyridines

According to the method described by García-Frutos et al [41], to a solution of 5-bromo-1*H*-pyrrolo[2,3-*b*]pyridine or 5-methoxy-1*H*-pyrrolo[2,3-*b*]pyridine [42] (1 equiv) in acetone (11 mL/mmol), KOH (1.5 equiv), tetrabutylammonium bisulfate (Bu₄N⁺HSO₄[−], 0.08 equiv), and the corresponding alkyl or benzyl halide (1.2 equiv)

was added under argon. The reaction was stirred at 75 °C for 2–5 h, monitoring the evolution of the reaction by TLC. When completed, it was cooled down to rt and water (10 mL/mmol) was added. Then, products were extracted with CH₂Cl₂ (3 × 30 mL/mmol) and the organic layer dried with Na₂SO₄ (anh.), filtered, and evaporated. The isolated product was purified by automatized column flash chromatography, using ethyl acetate/*n*-hexane mixtures as eluent, obtaining pure products as yellow oils.

4.10. 1-benzyl-5-bromo-1H-pyrrolo[2,3-*b*]pyridine (**9**)

According to the General Method for the *N*1-alkylation of 1*H*-pyrrolo[2,3-*b*]pyridines, 5-bromo-1*H*-pyrrolo[2,3-*b*]pyridine (350 mg, 1.78 mmol) [KOH (168 mg, 2.70 mmol), Bu₄N⁺HSO₄⁻ (51 mg, 0.15 mmol), benzyl bromide (252 μL, 2.13 mmol)] yielded **9** (506 mg, 99%) with spectral data according to literature [83].

4.11. 5-bromo-1-butyl-1H-pyrrolo[2,3-*b*]pyridine (**10**)

According to the General Method for the *N*1-alkylation of 1*H*-pyrrolo[2,3-*b*]pyridines, 5-bromo-1*H*-pyrrolo[2,3-*b*]pyridine (350 mg, 1.78 mmol) [KOH (168 mg, 2.70 mmol), Bu₄N⁺HSO₄⁻ (51 mg, 0.15 mmol), 1-iodobutane (243 μL, 2.13 mmol)] yielded **10** (452 mg, 99%). ¹H NMR (300 MHz, acetone-*d*₆) δ 8.33 (d, 1H, *J* = 2.1 Hz, H6), 8.05 (d, 1H, *J* = 2.1 Hz, H4), 7.42 (d, 1H, *J* = 3.6 Hz, H2), 6.42 (d, 1H, *J* = 3.6 Hz, H3), 4.26 (t, 2H, *J* = 7.2 Hz, NCH₂), 1.85–1.73 (m, 2H, NCH₂CH₂), 1.34–1.18 (m, 2H, CH₂CH₃), 0.87 (t, 3H, *J* = 7.5 Hz, CH₃).

4.12. 5-bromo-1-(pro-2-yn-1-yl)-1H-pyrrolo[2,3-b]pyridine (**11**)

According to the General Method for the *N1*-alkylation of 1H-pyrrolo[2,3-*b*]pyridines, 5-bromo-1H-pyrrolo[2,3-*b*]pyridine (400 mg, 2.03 mmol) [KOH (92 mg, 3.09 mmol), Bu₄N⁺HSO₄⁻ (59 mg, 0.17 mmol), 3-bromopro-1-yne (271 μL, 2.44 mmol)] yielded **11** (255 mg, 53%). ¹H NMR (300 MHz, acetone-*d*₆) δ 8.32 (d, 1H, *J* = 2.1 Hz, H6), 8.11 (d, 1H, *J* = 2.1 Hz, H4), 7.60 (d, 1H, *J* = 3.3 Hz, H2), 6.51 (d, 1H, *J* = 3.3 Hz, H3), 5.14 (d, 2H, *J* = 2.7 Hz, CH₂), 2.94 (t, 1H, *J* = 2.7 Hz, CH).

4.13. 1-benzyl-5-methoxy-1H-pyrrolo[2,3-*b*]pyridine (**12**)

According to the General Method for the *N1*-alkylation of 1H-pyrrolo[2,3-*b*]pyridines, 5-methoxy-1H-pyrrolo[2,3-*b*]pyridine [42] (80 mg, 0.54 mmol) [KOH (51 mg, 0.82 mmol), Bu₄N⁺HSO₄⁻ (16 mg, 0.04 mmol), benzyl bromide (77 μL, 0.65 mmol)] yielded **12** (128 mg, 99%). ¹H NMR (300 MHz, acetone-*d*₆) δ 8.10 (d, 1H, *J* = 2.7 Hz, H6), 7.52 (d, 1H, *J* = 2.7 Hz, H4), 7.42 (d, 1H, *J* = 3.3 Hz, H2), 7.33–7.18 (m, 5H, Ar), 6.43 (d, 1H, *J* = 3.3 Hz, H3), 5.49 (s, 2H, CH₂), 3.84 (s, 3H, CH₃).

4.14. General Method for the preparation of **1** derivatives **13–32**

According to the protocol of Miranda et al [84], with modifications [14]. Piperidine (1 equiv) or 40% aqueous dimethylamine (1 equiv) and 37% aqueous formaldehyde (1 equiv) were stirred under argon in acetic acid (glacial, 1–6 mL/mmol) for 10 min at room temperature to allow the formation of the corresponding iminium ion. Then, this solution was added to that of compound **3–12** (1 equiv) in acetic acid (glacial, 1–2

mL/mmol) at 0 °C and stirred for 5 min. Then, reaction was slowly warmed up to rt and stirred for 24 h more. When the reaction finished or did not evolve longer (TLC, basic alumina), it was interrupted by adding NaOH_{aq} (30%), up to pH 14 and extracted with neutralized CH₂Cl₂ (3 × 30 mL/mmol), dried with Na₂SO₄ (anh.), filtered, and evaporated. When necessary, purification was carried out by column flash chromatography using basic alumina as stationary phase and ethyl acetate/*n*-hexane mixtures as eluent. Pure products were isolated as oils and, to favor their water solubility and handling, their corresponding salts were formed by treatment with a solution of oxalic acid in dry ethyl acetate, according to a protocol recently described by our research group [14].

4.15. 1-(1-benzyl-1H-indol-3-yl)-N,N-dimethylmethanamine (**13**)

According to the General Method for the preparation of **1** analogues **13–32**, reaction of **3** (208 mg, 1 mmol) [dimethylamine (127 µL, 1 mmol) and formaldehyde (76 µL, 1 mmol)] yielded **13** as a yellow oil that did not require further purification (252 mg, 95%), with spectral data according to literature [79]. Compound was salinized to its oxalate salt: Mp 164–166 °C. ¹³C NMR (75.4 MHz, DMSO-*d*₆) δ 164.1, 137.7, 135.9, 132.1, 128.6, 128.0, 127.5, 127.1, 122.0, 120.0, 119.0, 110.7, 103.1, 50.7, 49.2, 41.2. Anal. C₁₈H₂₀N₂·C₂H₂O₄ (C, H, N).

4.16. 1-benzyl-3-(piperidin-1-ylmethyl)-1H-indole (**14**)

According to the General Method for the preparation of **1** analogues **13–32**, reaction of **3** (189 mg, 0.91 mmol) [piperidine (90 µL, 0.91 mmol) and formaldehyde (69 µL,

0.91 mmol)] yielded, after chromatographic purification, **14** as a yellow oil (230 mg, 83%), with spectral data according to literature [85]. Compound was salinized to its oxalate salt: Mp 181–183 °C. ^{13}C NMR (75.4 MHz, DMSO- d_6) δ 164.1, 137.7, 135.9, 131.9, 128.6, 128.1, 127.5, 127.1, 121.9, 119.9, 119.0, 110.6, 51.3, 50.5, 49.2, 22.7, 21.5. Anal. $\text{C}_{21}\text{H}_{24}\text{N}_2\cdot\text{H}_2\text{O}\cdot\text{C}_2\text{H}_2\text{O}_4$ (C, H, N).

4.17. 1-(1-butyl-1H-indol-3-yl)-N,N-dimethylmethanamine (**15**)

According to the General Method for the preparation of **1** analogues **13–32**, reaction of **4** (174 mg, 1 mmol) [dimethylamine (127 μL , 1 mmol) and formaldehyde (76 μL , 1 mmol)] yielded, after chromatographic purification, **15** as a yellow oil (79 mg, 34%).

^1H NMR (300 MHz, acetone- d_6) δ 7.76–7.63 (dm, 1H, J = 8.1 Hz, H4), 7.43–7.35 (dm, 1H, J = 8.1 Hz, H7), 7.23–7.08 (m, 2H, H2, H6), 7.01 (bdd, 1H, J = 8.1, 7.8 Hz, H5), 4.16 (t, 2H, J = 6.9 Hz, NCH_2CH_2), 3.56 (s, 2H, C3CH_2), 2.19 [s, 6H, $\text{N}(\text{CH}_3)_2$], 1.80 (m, 2H, NCH_2CH_2), 1.33 (m, 2H, CH_2CH_3), 0.92 (t, 3H, J = 7.2 Hz, CH_2CH_3).

Compound was salinized to its oxalate salt: Mp 142–144 °C. ^{13}C NMR (75.4 MHz, DMSO- d_6) δ 163.4, 135.8, 131.6, 127.7, 121.7, 119.7, 118.8, 110.3, 102.3, 50.8, 45.3, 41.1, 31.7, 19.4, 13.5. Anal. $\text{C}_{15}\text{H}_{22}\text{N}_2\cdot\text{H}_2\text{O}\cdot\text{C}_2\text{H}_2\text{O}_4$ (C, H, N).

4.18. 1-butyl-3-(piperidin-1-ylmethyl)-1H-indole (**16**)

According to the General Method for the preparation of **1** analogues **13–32**, reaction of **4** (170 mg, 0.98 mmol) [piperidine (97 μL , 0.98 mmol) and formaldehyde (74 μL , 0.98 mmol)] yielded, after chromatographic purification, **16** as a yellow oil (209 mg, 79%). ^1H NMR (300 MHz, acetone- d_6) δ 7.78–7.71 (dm, 1H, J = 7.8 Hz, H4), 7.41–

7.34 (dm, 1H, $J = 8.1$ Hz, H7), 7.20–7.09 (m, 2H, H2, H6), 7.03 (bt, 1H, $J = 7.8$ Hz, H5), 4.12 (t, 2H, $J = 7.1$ Hz, NCH₂CH₂), 3.61 (s, 2H, C3CH₂), 2.50–2.34 (m, 4H, H2'), 1.87–1.72 (m, 2H, NCH₂CH₂), 1.61–1.49 (m, 4H, H3'), 1.48–1.39 (m, 2H, H4'), 1.38–1.24 (m, 2H, CH₂CH₃), 0.92 (t, 3H, $J = 7.2$ Hz, CH₃). Compound was salinized to its oxalate salt: Mp 156–158 °C. ¹³C NMR (75.4 MHz, DMSO-*d*₆) δ 164.4, 135.8, 131.5, 128.0, 121.7, 119.7, 118.9, 110.3, 102.2, 51.2, 50.5, 45.4, 31.8, 22.6, 21.5, 19.5, 13.5. Anal. C₁₈H₂₆N₂·C₂H₂O₄ (C, H, N).

4.19. *N,N*-dimethyl-1-[1-(prop-2-yn-1-yl)-1H-indol-3-yl]methanamine (**17**)

According to the General Method for the preparation of **1** analogues **13–32**, reaction of **5** (167 mg, 1.08 mmol) [dimethylamine (136 μ L, 1.08 mmol) and formaldehyde (81 μ L, 1.08 mmol)] yielded **17** as a yellow oil that did not require further purification (228 mg, > 99%). ¹H NMR (300 MHz, acetone-*d*₆) δ 7.75–7.68 (dm, 1H, $J = 8.1$ Hz, H4), 7.50–7.44 (dm, 1H, $J = 8.4$ Hz, H7), 7.26 (s, 1H, H2), 7.20 (ddd, 1H, $J = 1.2, 7.8, 8.4$ Hz, H6), 7.07 (ddd, 1H, $J = 1.2, 8.1, 7.8$ Hz, H5), 5.02 (d, 2H, $J = 2.4$ Hz, NCH₂CCH), 3.59 (s, 2H, C3CH₂), 2.93 (t, 1H, $J = 2.4$ Hz, CH), 2.21 [s, 6H, N(CH₃)₂]. Compound was salinized to its oxalate salt: Mp 168–170 °C. ¹³C NMR (75.4 MHz, DMSO-*d*₆) δ 164.2, 135.6, 131.0, 127.9, 122.1, 120.2, 119.0, 110.5, 103.8, 78.8, 76.0, 50.8, 41.3, 35.3. Anal. C₁₄H₁₆N₂·C₂H₂O₄ (C, H, N).

4.20. 3-(piperidin-1-ylmethyl)-1-(prop-2-yn-1-yl)-1H-indole (**18**)

According to the General Method for the preparation of **1** analogues **13–32**, reaction of **5** (118 mg, 0.76 mmol) [piperidine (75 μ L, 0.76 mmol) and formaldehyde (58 μ L,

0.76 mmol)] yielded, after chromatographic purification, **18** as a yellow oil (191 mg, > 99%). ¹H NMR (300 MHz, acetone-*d*₆) δ 7.78–7.71 (dm, 1H, *J* = 8.1 Hz, H4), 7.49–7.41 (dm, 1H, *J* = 8.1 Hz, H7), 7.22 (s, 1H, H2), 7.19 (bdd, 1H, *J* = 7.8, 8.1, H6), 7.07 (bdd, 1H, *J* = 7.8, 8.1 Hz, H5), 5.01 (d, 2H, *J* = 2.4 Hz, NCH₂CCH), 3.61 (s, 2H, C3CH₂), 2.92 (t, 1H, *J* = 2.4 Hz, CH), 2.47–2.29 (m, 4H, H2'), 1.57–1.46 (m, 4H, H3'), 1.45–1.35 (m, 2H, H4'). Compound was salinized to its oxalate salt: Mp 162–164 °C. ¹³C NMR (75.4 MHz, DMSO-*d*₆) δ 164.1, 135.5, 131.1, 128.2, 122.1, 120.2, 119.0, 110.5, 103.2, 78.8, 76.1, 51.3, 50.3, 35.3, 22.6, 21.4. Anal. C₁₇H₂₀N₂·H₂O·C₂H₂O₄ (C, H, N)

4.21. 1-(1-benzyl-5-chloro-1H-indol-3-yl)-N,N-dimethylmethanamine (**19**)

According to the General Method for the preparation of **1** analogues **13–32**, reaction of **6** (219 mg, 0.91 mmol) [dimethylamine (115 μL, 0.91 mmol) and formaldehyde (68 μL, 0.91 mmol)] yielded **19** as a yellow oil that did not require further purification (269 mg, > 99%). ¹H NMR (300 MHz, acetone-*d*₆) δ 7.79 (bd, 1H, *J* = 2.1 Hz, H4), 7.36–7.24 (m, 5H, Ar), 7.17–7.14 (m, 2H, Ar), 7.11 (dd, 1H, *J* = 2.1, 8.1 Hz, H6), 5.34 (s, 2H, NCH₂Ph), 3.57 (s, 2H, C3CH₂), 2.22 [s, 6H, N(CH₃)₂]. Compound was salinized to its oxalate salt: Mp 177–179 °C. ¹³C NMR (75.4 MHz, DMSO-*d*₆) δ 164.3, 137.4, 135.7, 134.4, 133.5, 129.1, 128.6, 127.6, 127.0, 124.9, 121.9, 118.5, 50.6, 49.4, 41.3. Anal. C₁₈H₁₉ClN₂·C₂H₂O₄ (C, H, N).

4.22. 1-benzyl-5-chloro-3-(piperidin-1-ylmethyl)-1H-indole (**20**)

According to the General Method for the preparation of **1** analogues **13–32**, reaction of **6** (219 mg, 0.91 mmol) [piperidine (90 μ L, 0.91 mmol) and formaldehyde (69 μ L, 0.91 mmol)] yielded, after chromatographic purification, **20** as a yellow oil (278 mg, 91%). ^1H NMR (300 MHz, acetone- d_6) δ 7.77 (bd, 1H, J = 2.1 Hz, H4), 7.37–7.16 (m, 7H, Ar), 7.08 (dd, 1H, J = 2.1, 8.7 Hz, H6), 5.38 (s, 2H, NCH₂Ph), 3.60 (s, 2H, C3CH₂), 2.48–2.31 (m, 4H, H2'), 1.60–1.47 (m, 4H, H3'), 1.46–1.36 (m, 2H, H4'). Compound was salinized to its oxalate salt: Mp 198–200 °C. ^{13}C NMR (75.4 MHz, DMSO- d_6) δ 164.0, 137.4, 134.4, 133.4, 129.3, 128.6, 127.6, 127.1, 124.8, 121.9, 118.5, 112.3, 51.4, 50.3, 49.4, 22.7, 21.6. Anal. C₂₁H₂₃ClN₂·C₂H₂O₄ (C, H, N).

4.23. 1-(1-butyl-5-chloro-1H-indol-3-yl)-N,N-dimethylmethanamine (**21**)

According to the General Method for the preparation of **1** analogues **13–32**, reaction of **7** (168 mg, 0.81 mmol) [dimethylamine (102 μ L, 0.81 mmol) and formaldehyde (61 μ L, 0.81 mmol)] yielded **21** as a yellow oil that did not require further purification (210 mg, > 99%). ^1H NMR (300 MHz, acetone- d_6) δ 7.71 (d, 1H, J = 2.1 Hz, H4), 7.38 (d, 1H, J = 8.7 Hz, H7), 7.21 (s, 1H, H2), 7.11 (dd, 1H, J = 2.1, 8.7 Hz, H6), 4.14 (t, 2H, J = 7.2 Hz, NCH₂CH₂), 3.53 (s, 2H, C3CH₂), 2.18 [s, 6H, N(CH₃)₂], 1.84–1.71 (m, 2H, NCH₂CH₂), 1.38–1.22 (m, 2H, CH₂CH₃), 0.93 (t, 3H, J = 7.2 Hz, CH₂CH₃).

Compound was salinized to its oxalate salt: Mp 150–152 °C. ^{13}C NMR (75.4 MHz, D₂O + acetone- d_6) δ 165.3, 135.0, 133.7, 128.8, 126.0, 122.7, 118.0, 112.5, 101.6, 52.2, 46.4, 41.8, 31.8, 19.7, 13.2. Anal. C₁₅H₂₁ClN₂·H₂O·C₂H₂O₄ (C, H, N).

4.24. 1-butyl-5-chloro-3-(piperidin-1-ylmethyl)-1H-indole (**22**)

According to the General Method for the preparation of **1** analogues **13–32**, reaction of **7** (212 mg, 1.02 mmol) [piperidine (101 μ L, 1.02 mmol) and formaldehyde (76 μ L, 1.02 mmol)] yielded, after chromatographic purification, **22** as a yellow oil (287 mg, 92%). ^1H NMR (300 MHz, acetone- d_6) δ 7.78 (d, 1H, J = 2.1 Hz, H4), 7.35 (d, 1H, J = 8.7 Hz, H7), 7.16 (s, 1H, H2), 7.12 (dd, 1H, J = 2.1, 8.7 Hz, H6), 4.09 (t, 2H, J = 7.2 Hz, NCH_2CH_2), 3.57 (s, 2H, C3CH_2), 2.47–2.30 (m, 4H, H2'), 1.84–1.69 (m, 2H, NCH_2CH_2), 1.60–1.48 (m, 4H, H3'), 1.47–1.37 (m, 2H, H4'), 1.36–1.22 (m, 2H, CH_2CH_3), 0.91 (t, 3H, J = 7.5 Hz, CH_3). Compound was salinized to its oxalate salt: Mp 184–186 $^\circ\text{C}$. ^{13}C NMR (75.4 MHz, DMSO- d_6) δ 164.5, 134.3, 133.0, 129.1, 124.6, 121.6, 118.3, 111.9, 102.3, 54.9, 51.1, 50.1, 45.6, 31.7, 22.6, 21.5, 19.4, 13.5. Anal. $\text{C}_{18}\text{H}_{25}\text{ClN}_2\cdot\text{C}_2\text{H}_2\text{O}_4$ (C, H, N).

4.25. 1-[5-chloro-1-(prop-2-yn-1-yl)-1H-indol-3-yl]-N,N-dimethylmethanamine (**23**)

According to the General Method for the preparation of **1** analogues **13–32**, reaction of **8** (121 mg, 0.64 mmol) [dimethylamine (81 μ L, 0.64 mmol) and formaldehyde (48 μ L, 0.64 mmol)] yielded **23** as a yellow oil that did not require further purification (149 mg, 95%). ^1H NMR (300 MHz, acetone- d_6) δ 7.72 (d, 1H, J = 2.1 Hz, H4), 7.48 (d, 1H, J = 8.7 Hz, H7), 7.32 (s, 1H, H2), 7.18 (dd, 1H, J = 2.1, 8.7 Hz, H6), 5.04 (d, 2H, J = 2.4 Hz, NCH_2CCH), 3.54 (s, 2H, C3CH_2), 2.96 (t, 1H, J = 2.4 Hz, CH), 2.19 [s, 6H, $\text{N}(\text{CH}_3)_2$]. Compound was salinized to its oxalate salt: Mp 170–172 $^\circ\text{C}$. ^{13}C NMR (75.4 MHz, DMSO- d_6) δ 164.1, 134.1, 132.5, 129.1, 125.1, 122.1, 118.6, 112.2, 104.1, 78.5, 76.3, 50.7, 41.5, 35.6. Anal. $\text{C}_{14}\text{H}_{15}\text{ClN}_2\cdot\text{C}_2\text{H}_2\text{O}_4$ (C, H, N).

4.26. 5-chloro-3-(piperidin-1-ylmethyl)-1-(prop-2-yn-1-yl)-1H-indole (**24**)

According to the General Method for the preparation of **1** analogues **13–32**, reaction of **8** (117 mg, 0.62 mmol) [piperidine (61 μ L, 0.62 mmol) and formaldehyde (47 μ L, 0.62 mmol)] yielded, after chromatographic purification, **24** as a yellow oil (175 mg, > 99%). ^1H NMR (300 MHz, acetone- d_6) δ 7.76 (d, 1H, J = 2.1 Hz, H4), 7.47 (d, 1H, J = 8.7 Hz, H7), 7.29 (s, 1H, H2), 7.17 (dd, 1H, J = 2.1, 8.7, H6), 5.03 (d, 2H, J = 2.4 Hz, NCH_2CCH), 3.57 (s, 2H, C3CH_2), 2.95 (t, 1H, J = 2.4 Hz, CH), 2.48–2.28 (m, 4H, H2'), 1.57–1.47 (m, 4H, H3'), 1.46–1.36 (m, 2H, H4'). Compound was salinized to its oxalate salt: Mp 187–189 $^\circ\text{C}$. ^{13}C NMR (75.4 MHz, DMSO- d_6) δ 164.3, 134.1, 132.7, 129.4, 125.2, 122.1, 118.6, 112.2, 103.3, 78.5, 76.4, 51.3, 49.9, 35.6, 22.6, 21.5. Anal. $\text{C}_{17}\text{H}_{19}\text{ClN}_2\cdot\text{C}_2\text{H}_2\text{O}_4$ (C, H, N).

4.27. 1-(1-benzyl-5-bromo-1H-pyrrolo[2,3-b]pyridin-3-yl)-N,N-dimethylmethanamine (**25**)

According to the General Method for the preparation of **1** analogues **13–32**, reaction of **9** (134 mg, 0.47 mmol) [dimethylamine (60 μ L, 0.47 mmol) and formaldehyde (34 μ L, 0.47 mmol)] yielded **25** as a greenish oil that did not require further purification (161 mg, > 99%). ^1H NMR (300 MHz, acetone- d_6) δ 8.31 (d, 1H, J = 2.1 Hz, H6), 8.24 (d, 1H, J = 2.1 Hz, H4), 7.41 (s, 1H, H2), 7.33–7.20 (m, 5H, Ar), 5.47 (s, 2H, NCH_2Ph), 3.52 (s, 2H, C3CH_2), 2.17 [s, 6H, $\text{N}(\text{CH}_3)_2$]. Compound was salinized to its oxalate salt: Mp 203–205 $^\circ\text{C}$. ^{13}C NMR (75.4 MHz, D_2O + acetone- d_6) δ 166.0, 145.5, 144.3, 137.2, 134.4, 130.8, 129.3, 128.4, 127.5, 122.5, 112.6, 101.6, 51.9, 48.7, 42.0. Anal. $\text{C}_{17}\text{H}_{18}\text{BrN}_3\cdot\text{C}_2\text{H}_2\text{O}_4$ (C, H, N).

4.28. 1-benzyl-5-bromo-3-(piperidin-1-ylmethyl)-1H-pyrrolo[2,3-b]pyridine (**26**)

According to the General Method for the preparation of **1** analogues **13–32**, reaction of **9** (280 mg, 0.98 mmol) [piperidine (96 μ L, 0.98 mmol) and formaldehyde (73 μ L, 0.98 mmol)] yielded, after chromatographic purification, **26** as a yellow oil (372 mg, > 99%). ^1H NMR (300 MHz, acetone- d_6) δ 8.31 (d, 1H, J = 2.4 Hz, H6), 8.27 (d, 1H, J = 2.4 Hz, H4), 7.38 (s, 1H, H2), 7.33–7.19 (m, 5H, Ar), 5.46 (s, 2H, NCH_2Ph), 3.55 (s, 2H, C3CH_2), 2.40–2.29 (m, 4H, H2'), 1.55–1.45 (m, 4H, H3'), 1.44–1.33 (m, 2H, H4'). Compound was salinized to its oxalate salt: Mp 214–216 $^\circ\text{C}$. ^{13}C NMR (75.4 MHz, DMSO- d_6) δ 164.0, 145.4, 143.4, 137.5, 133.3, 130.0, 128.6, 127.6, 127.3, 121.9, 111.8, 51.5, 50.2, 47.5, 22.8, 21.6. Anal. $\text{C}_{20}\text{H}_{22}\text{BrN}_3\cdot\text{C}_2\text{H}_2\text{O}_4$ (C, H, N).

4.29. 1-(5-bromo-1-butyl-1H-pyrrolo[2,3-b]pyridin-3-yl)-N,N-dimethylmethanamine (**27**)

According to the General Method for the preparation of **1** analogues **13–32**, reaction of **10** (174 mg, 0.69 mmol) [dimethylamine (87 μ L, 0.69 mmol) and formaldehyde (52 μ L, 0.69 mmol)] yielded **27** as a greenish oil that did not require further purification (198 mg, 93%). ^1H NMR (300 MHz, acetone- d_6) δ 8.27 (d, 1H, J = 2.4 Hz, H6), 8.19 (d, 1H, J = 2.4 Hz, H4), 7.38 (s, 1H, H2), 4.25 (t, 2H, J = 6.9 Hz, NCH_2CH_2), 3.52 (s, 2H, C3CH_2), 2.17 [s, 6H, $\text{N}(\text{CH}_3)_2$], 1.87–1.75 (m, 2H, NCH_2CH_2), 1.35–1.20 (m, 2H, CH_2CH_3), 0.93 (t, 3H, J = 7.2 Hz, CH_2CH_3). Compound was salinized to its oxalate salt: Mp 181–183 $^\circ\text{C}$. ^{13}C NMR (75.4 MHz, DMSO- d_6) δ 164.2, 145.4, 143.1, 133.3, 129.9, 121.6, 111.5, 101.8, 50.9, 43.9, 41.5, 31.6, 19.3, 13.5. Anal. $\text{C}_{14}\text{H}_{20}\text{BrN}_3\cdot\text{C}_2\text{H}_2\text{O}_4$ (C, H, N).

4.30. 5-bromo-1-butyl-3-(piperidin-1-ylmethyl)-1H-pyrrolo[2,3-b]pyridine (**28**)

According to the General Method for the preparation of **1** analogues **13–32**, reaction of **10** (125 mg, 0.49 mmol) [piperidine (49 μ L, 0.49 mmol) and formaldehyde (37 μ L, 0.49 mmol)] yielded, after chromatographic purification, **28** as a yellow oil (175 mg, > 99%). ^1H NMR (300 MHz, acetone- d_6) δ 8.27 (d, 1H, J = 2.1 Hz, H6), 8.22 (d, 1H, J = 2.1 Hz, H4), 7.35 (s, 1H, H2), 4.24 (t, 2H, J = 7.2 Hz, NCH_2CH_2), 3.55 (s, 2H, C3CH_2), 2.42–2.28 (m, 4H, H2'), 1.88–1.75 (m, 2H, NCH_2CH_2), 1.57–1.45 (m, 4H, H3'), 1.44–1.35 (m, 2H, H4'), 1.36–1.21 (m, 2H, CH_2CH_3), 0.90 (t, 3H, J = 7.2 Hz, CH_3). Compound was salinized to its oxalate salt: Mp 208–210 $^\circ\text{C}$. ^{13}C NMR (75.4 MHz, DMSO- d_6) δ 164.3, 145.4, 143.0, 133.4, 129.7, 121.9, 111.5, 101.2, 54.9, 51.3, 50.1, 43.8, 31.5, 22.7, 21.5, 19.3, 13.4. Anal. $\text{C}_{17}\text{H}_{24}\text{BrN}_3\cdot\text{C}_2\text{H}_2\text{O}_4$ (C, H, N).

4.31. 1-[5-bromo-1-(prop-2-yn-1-yl)-1H-pyrrolo[2,3-b]pyridin-3-yl]-N,N-dimethylmethanamine (**29**)

According to the General Method for the preparation of **1** analogues **13–32**, reaction of **11** (143 mg, 0.61 mmol) [dimethylamine (77 μ L, 0.61 mmol) and formaldehyde (46 μ L, 0.61 mmol)] yielded, after chromatographic purification, **29** as a yellow oil (114 mg, 64%). ^1H NMR (300 MHz, acetone- d_6) δ 8.31 (d, 1H, J = 2.4 Hz, H6), 8.24 (d, 1H, J = 2.4 Hz, H4), 7.51 (s, 1H, H2), 5.10 (d, 2H, J = 2.4 Hz, NCH_2CCH), 3.56 (s, 2H, C3CH_2), 2.93 (t, 1H, J = 2.4 Hz, CH), 2.19 [s, 6H, $\text{N}(\text{CH}_3)_2$]. Compound was salinized to its oxalate salt: Mp 179–181 $^\circ\text{C}$. ^{13}C NMR (75.4 MHz, DMSO- d_6) δ 164.1,

145.0, 143.6, 132.6, 130.3, 121.8, 112.1, 103.1, 78.7, 75.9, 50.8, 41.6, 33.7. Anal.

$C_{13}H_{14}BrN_3 \cdot C_2H_2O_4$ (C, H, N).

4.32. 5-bromo-3-(piperidin-1-ylmethyl)-1-(prop-2-yn-1-yl)-1H-pyrrolo[2,3-b]pyridine (30)

According to the General Method for the preparation of **1** analogues **13–32**, reaction of **11** (113 mg, 0.48 mmol) [piperidine (47 μ L, 0.48 mmol) and formaldehyde (36 μ L, 0.48 mmol)] yielded, after chromatographic purification, **30** as a yellow oil (143 mg, 89%). 1H NMR (300 MHz, acetone- d_6) δ 8.31 (d, 1H, J = 2.1 Hz, H6), 8.28 (d, 1H, J = 2.1 Hz, H4), 7.49 (s, 1H, H2), 5.10 (d, 2H, J = 2.4 Hz, NCH_2CCH), 3.60 (s, 2H, $C3CH_2$), 2.92 (t, 1H, J = 2.4 Hz, CH), 2.43–2.31 (m, 4H, H2'), 1.58–1.47 (m, 4H, H3'), 1.46–1.37 (m, 2H, H4'). Compound was salinized to its oxalate salt: Mp 198–200 $^{\circ}C$. ^{13}C NMR (75.4 MHz, DMSO- d_6) δ 163.9, 145.0, 143.4, 132.6, 130.1, 122.0, 112.0, 78.6, 75.9, 51.5, 50.2, 33.6, 22.8, 21.5. Anal. $C_{16}H_{18}BrN_3 \cdot C_2H_2O_4$ (C, H, N).

4.33. 1-(1-benzyl-5-methoxy-1H-pyrrolo[2,3-b]pyridin-3-yl)-N,N-dimethylmethanamine (31)

According to the General Method for the preparation of **1** analogues **13–32**, reaction of **12** (73 mg, 0.31 mmol) [dimethylamine (39 μ L, 0.31 mmol) and formaldehyde (23 μ L, 0.31 mmol)] yielded **31** as a yellow oil that did not require further purification (67 mg, 74%). 1H NMR (300 MHz, acetone- d_6) δ 8.03 (d, 1H, J = 2.7 Hz, H6), 7.63 (d, 1H, J = 2.7 Hz, H4), 7.33 (s, 1H, H2), 7.30–7.22 (m, 5H, Ar), 5.45 (s, 2H, NCH_2Ph), 3.86 (s, 3H, OCH_3), 3.54 (s, 2H, $C3CH_2$), 2.18 [s, 6H, $N(CH_3)_2$]. Compound was

salinized to its oxalate salt: Mp 187–189 °C. ^{13}C NMR (75.4 MHz, DMSO- d_6) δ 164.3, 151.5, 142.3, 138.0, 133.8, 132.3, 128.6, 127.4, 127.2, 119.9, 110.3, 101.7, 56.1, 51.0, 47.4, 41.3. Anal. $\text{C}_{18}\text{H}_{21}\text{N}_3\text{O}\cdot\text{C}_2\text{H}_2\text{O}_4$ (C, H, N).

4.34. 1-benzyl-5-methoxy-3-(piperidin-1-ylmethyl)-1H-pyrrolo[2,3-b]pyridine (**32**)

According to the General Method for the preparation of **1** analogues **13–32**, reaction of **12** (60 mg, 0.25 mmol) [piperidine (25 μL , 0.25 mmol) and formaldehyde (19 μL , 0.25 mmol)] yielded, after chromatographic purification, **32** as a yellow oil (66 mg, 78%). ^1H NMR (300 MHz, acetone- d_6) δ 8.02 (d, 1H, J = 2.4 Hz, H6), 7.67 (d, 1H, J = 2.4 Hz, H4), 7.33–7.20 (m, 5H, Ar), 7.30 (s, 1H, H2), 5.44 (s, 2H, NCH_2Ph), 3.86 (s, 3H, OCH_3), 3.57 (s, 2H, C3CH_2), 2.45–2.29 (m, 4H, H2'), 1.57–1.46 (m, 4H, H3'), 1.45–1.35 (m, 2H, H4'). Compound was salinized to its oxalate salt: Mp 195–197 °C. ^{13}C NMR (75.4 MHz, DMSO- d_6) δ 164.3, 151.5, 142.3, 138.0, 133.7, 132.4, 128.6, 127.5, 127.3, 120.2, 110.3, 56.1, 51.2, 50.4, 47.5, 22.7, 21.5. Anal. $\text{C}_{21}\text{H}_{25}\text{N}_3\text{O}\cdot\text{C}_2\text{H}_2\text{O}_4$ (C, H, N).

4.35. Molecular modeling

The conformations of compounds **19** and **32** were obtained in Spartan version 14 (Wavefunction, Inc.; Irvine, CA) by Monte Carlo, optimizing the most stable under a HF method-based *ab initio* base 6-31G*. To run the docking experiments, the 3D structure of PP2A deposited in the protein data bank (www.rcsb.org; PDB ID: 2IE4, removing the co-crystallized inhibitor OA and the water molecules) was selected [49],

and the calculations carried out in the Molegro Virtual Docker v. 3.2.1 software. The algorithm used for ranking the best energies was MolDock Score [86].

4.36. Data analysis

To calculate the necessary sample size (n) for each experiment, taking a confidence interval (Z) of 95% and an error margin admitted (e) of 5%, we applied the formula $n = Z^2 \cdot \sigma^2 / e^2$, where the averaged standard deviation (σ) in our similar previous experiments using neuroblastoma cells was 0.04. Thus, a sample size of a minimum of three experiments was necessary. Comparisons between control and test groups were executed by an one-way analysis of variance (ANOVA), followed by Dunnett or Newman—Keuls post hoc test, using the GraphPad Prism 5.0 for Mac OS X software, and considered statistical different when $p \leq 0.05$.

4.37. Cell cultures

SH-SY5Y cells, purchased from ATCC (Barcelona, Spain; cat#CRL-2266), were maintained in an incubator at 37 °C under moisture-saturated air atmosphere with 5% CO₂, similarly to what has been described [87]. After confirming the cell batches are micoplasma-free by the Mycoplasma detection kit QuickTest (Bimake.com, cat.# B39032, Houston, TX, USA), the SH-SY5Y cells, in a low number of passage, were seeded with MEM-F12 medium in a density that depended on the experiments planned, according to what were recently described [14].

Bovine chromaffin cells were isolated from adrenal glands of calves sacrificed in a local slaughterhouse, and cultured according to the protocol described below for

patch-clamp experiments [88]. All the experiments were conducted in sterile conditions.

4.38. Neuroprotection and phosphatase activity assays

Twenty-four hours after seeding in 48-well plates, SH-SY5Y neuroblastoma cells were preincubated with compounds, used in their white, crystalline, oxalate form, at the concentration expressed in each experiment for 24 h. Then, toxic stimuli (OA or R/O) were applied to cells, together with the compounds at the same concentration. For the phosphatase activity experiments, SH-SY5Y cells were incubated in those conditions for 18 h, after which cell medium was removed and 100 μ L of a 1:1 mixture of the phosphatase activity buffer (Phosphatase Assay Kit, cat.#786–453, G-Bioscience, St. Louis, MO) and pNPP 10 mM were added, according to the protocol indicated by the manufacturer, allowing the phosphate hydrolysis reaction at 37 °C for 30 min in dark. Supernatants were transferred to a 96-well plate to measure the absorbance of each well at 405 nm in a multi-well plate spectrophotometric reader (FluoStar Optima, BMG, Germany), whereby the more absorbance obtained at that wavelength, the more phosphatase activity executed by the cells. Cell non-treated with OA and compounds defined the maximal phosphatase activity, normalized to 100%. The selective PP2A inhibitor OA reduced phosphatase activity by 27%, and the presence of compounds along OA mitigated such decay in the activity in a percentage expressed in Table 1, thus considered % Recovery. For the neuroprotection experiments, the time of incubation of the toxic stimulus plus compounds was 20 to 24 h, after which MTT was applied to cells at the concentration of 1.2 mM and incubated for 2 h in dark. Media were removed and the

precipitated, purple-colored formazan, generated by the reduction of MTT, was dissolved with 0.3 mL of DMSO. Solutions were transferred to a 96-well plate to measure the absorbance of each well at 540 nm in a multi-well plate reader, whereby the more purple absorbance, the more cell viability. Cells non-treated with toxic stimuli and compounds defined the maximal cell viability, normalized to 100%. The selective PP2A inhibitor OA and the stressor cocktail R/O reduced cell viability by 30% and 38%, respectively, and the presence of compounds along the toxic stimulus mitigated such decay in the viability in a percentage expressed in Table 3, thus considered % Protection.

4.39. Western-blot analyses

The phosphorylation rate at Tau in SH-SY5Y neuroblastoma cells was assessed by western-blot with the anti-Human PHF-Tau monoclonal antibody AT8 (ref. #MN1020, ThermoFisher Scientific, MA, USA), according to manufacturer guidelines, with slight modifications (supplementary data). For that purpose, proteins of the SH-SY5Y culture were extracted with Mammalian Protein Extraction Reagent (ThermoFisher Scientific, MA, USA) under vortex shaking at 4 °C for 15 min, in presence of the Halt Protease Inhibitor Cocktail (Thermo Scientific, USA) and a Tyr phosphatases inhibitor (NaVO_3 1 mM). After centrifugation at 12 000 rpm and 4 °C for 15 min, cytosolic proteins were collected from the supernatant. Proteins were denaturalized in Laemli 5x buffer at 95 °C for 5 min. Proteins were charged and subjected to current clamped electrophoresis (SDS-PAGE, 12%), and transferred to the polyvinylidene fluoride Immobilon-P Transfer (Millipore, USA). Membranes were blocked for 2 h in TRIS-saline buffer solution with 0.05% Tween-20 and 4% BSA,

then incubated with the primary antibody anti-pTau at rt for 2 h (AT8, pSer 202 / pThr 205, 1:1 000). Data were normalized compared to β -actine (1: 100 000, Merck) bands. After washing up the membranes several times with TRIS-Tween 20 (1%) solution, they were incubated with the peroxidase-conjugated secondary antibody (1: 10 000, Santa Cruz Biotech.) several times at rt for 1 h. Finally, membranes were revealed by chemoluminescence with the ECL Select Western Blotting Detection Reagent (GE Healthcare, Barcelona, Spain). Optical densitometry of bands were quantified by Scion Image Alpha 4.0.3.2 software (Maryland, USA).

4.40. Fluorescence-based cell Ca^{2+} increases measurements

SH-SY5Y cells, cultured in clear-bottomed, black 96-well plates, were used when the 100% of confluence was reached, normally 36 to 72 h after seeding. The Ca^{2+} -sensitive Fluo-4/AM (acetoxymethylester) dye at 10 μM was charged to cells together with pluronic acid 0.2% to facilitate the entry of the fluorescent dye. After washing the cells out of the charge buffer, the depolarization (70 mM K^+)-induced cell Ca^{2+} increases were real-time monitored in presence of the compounds at 1 μM , according to a method recently described [14].

4.41. Patch-Clamp experiments in bovine chromaffin cells

Bovine chromaffin cells with 2–4 days of culture were used at rt to run the experiments. Ca^{2+} currents (I_{Ca}) were monitored by patch-clamp methodology in voltage-clamped cells under whole-cell configuration [89]. Cells were continuously superfused with Krebs-HEPES solution with the following composition, in mM: 145

NaCl, 5.6 KCl, 1.2 MgCl₂, 2 CaCl₂, 11 glucose, and 10 HEPES (pH 7.4, NaOH).

Cells were dialyzed with an intracellular solution of the following composition, in mM: 100 Cs glutamate, 14 EGTA, 20 tetraethyl ammonium chloride, 10 NaCl, 5 ATP-Mg, 0.3 GTP-Na, and 20 HEPES (pH 7.3, CsOH). Whole-cell records were performed with pipettes that showed a resistance of 5-7 MΩ, which were built on the headstage of an EPC-9 patch-clamp amplifier, with cancellation of capacitative transients and compensation of series resistance. Data were obtained with a sample frequency of 20 kHz, according to what acquired with the PULSE v8.74 software (HEKA Elektronik). Cells plated in coverslips were deposited in a chamber on an inverted microscope. To replace external solutions, multibarrel pipette-coupled miniature solenoid valves were used, placing the common outlet within 100 μm of the cell to be patched, choosing a flow rate of 1 mL/min. Resting potential was held at –80 mV and cells were challenged to 50 ms depolarizing pulses from –60 mV to +70 mV every 20 s, with 10 mV steps (Intensity-Voltage (I-V) curve). After disrupting the clamped membrane by aspiration, a control I-V curve was applied. Next, cells were exposed to compounds and 3 min after another I-V curve was applied to the cell.

Conflicts of interest

Authors declare no conflicts of interest

Acknowledgments

This work was supported by the following grants: Proyectos de Investigación en Salud (PI13/00789 and PI16/01041, IS Carlos III to C.d.I.R; co-funded by FEDER),

SAF2016/78892-R, Ministerio de Economía y Competitividad, Spain, to L.G.). R.L.C and R.L.A thank Universidad Autónoma de Madrid (UAM) for predoctoral fellowships. C.N. thanks Comunidad de Madrid for postdoctoral fellowships (Youth Employment Initiative). We thank the continued support of Prof. Antonio G. García (UAM) and Fundación Teófilo Hernando (Madrid, Spain).

Appendix A. Supplementary data

Supplementary data related to this article can be found at

<https://doi.org/10.1016/j.ejmech.2018.xx.xxx>

References

- [1] Yang, T., Moreira, W., Nyantakyi, S. A., Chen, H., Aziz, D. B., Go, M. L., and Dick, T., Amphiphilic Indole Derivatives as Antimycobacterial Agents: Structure-Activity Relationships and Membrane Targeting Properties, *J. Med. Chem.* 60 (2017) 2745–2763.
- [2] Nepali, K., Lee, H. Y., Lai, M. J., Ojha, R., Wu, T. Y., Wu, G. X., Chen, M. C., and Liou, J. P., Ring-opened tetrahydro-gamma-carbolines display cytotoxicity and selectivity with histone deacetylase isoforms, *Eur. J. Med. Chem.* 127 (2017) 115–127.
- [3] Nirogi, R., Shinde, A., Kambhampati, R. S., Mohammed, A. R., Saraf, S. K., Badange, R. K., Bandyala, T. R., Bhatta, V., Bojja, K., Reballi, V., Subramanian, R., Benade, V., Palacharla, R. C., Bhyrapuneni, G., Jayarajan, P., Goyal, V., and Jasti, V., Discovery and Development of 1-[(2-

- Bromophenyl)sulfonyl]-5-methoxy-3-[(4-methyl-1-piperazinyl)methyl]-1H-indole Dimesylate Monohydrate (SUVN-502): A Novel, Potent, Selective and Orally Active Serotonin 6 (5-HT₆) Receptor Antagonist for Potential Treatment of Alzheimer's Disease, *J. Med. Chem.* 60 (2017) 1843–1859.
- [4] Musella, S., di Sarno, V., Ciaglia, T., Sala, M., Spensiero, A., Scala, M. C., Ostacolo, C., Andrei, G., Balzarini, J., Snoeck, R., Novellino, E., Campiglia, P., Bertamino, A., and Gomez-Monterrey, I. M., Identification of an indole-based derivative as potent and selective varicella zoster virus (VZV) inhibitor, *Eur. J. Med. Chem.* 124 (2016) 773–781.
- [5] Bitler, B. G., Aird, K. M., Garipov, A., Li, H., Amatangelo, M., Kossenkova, A. V., Schultz, D. C., Liu, Q., Shih, M., Conejo-Garcia, J. R., Speicher, D. W., and Zhang, R., Synthetic lethality by targeting EZH2 methyltransferase activity in ARID1A-mutated cancers, *Nat. Med.* 21 (2015) 231–238.
- [6] Orechov, A., and Norkina, S., Über die Alkaloide von *Arundo Donax* L, *Ber. Deutsch. Chem. Gesells.* 68 (1935) 436–437.
- [7] Froldi, G., Silvestrin, B., Dorigo, P., and Caparrotta, L., Gramine: a vasorelaxing alkaloid acting on 5-HT_{2A} receptors, *Planta Med.* 70 (2004) 373–375.
- [8] Niemeyer, H. M., and Roveri, O. A., Effects of gramine on energy metabolism of rat and bovine mitochondria, *Biochem. Pharmacol.* 33 (1984) 2973–2979.
- [9] Olgen, S., Kilic-Kurt, Z., Sener, F., Isgor, Y. G., and Coban, T., Evaluation of novel aminomethyl indole derivatives as Src kinase inhibitors and antioxidant agents, *Chemotherapy* 57 (2011) 1–6.

- [10] Shukla, P. K., Gautam, L., Sinha, M., Kaur, P., Sharma, S., and Singh, T. P., Structures and binding studies of the complexes of phospholipase A2 with five inhibitors, *Biochim. Biophys. Acta* 1854 (2015) 269–277.
- [11] Pullagurla, M. R., Dukat, M., Setola, V., Roth, B., and Glennon, R. A., N1-benzenesulfonylgramine and N1-benzenesulfonylskatole: novel 5-HT₆ receptor ligand templates, *Bioorg. Med. Chem. Lett.* 13 (2003) 3355–3359.
- [12] Nakahata, N., Harada, Y., Tsuji, M., Kon-ya, K., Shizuri, Y., and Ohizumi, Y., Structure-activity relationship of gramine derivatives in Ca(2+) release from sarcoplasmic reticulum, *Eur. J. Pharmacol.* 382 (1999) 129–132.
- [13] Palmieri, A., Petrini, M., and Shaikh, R. R., Synthesis of 3-substituted indoles via reactive alkylideneindolenine intermediates, *Org. Biomol. Chem.* 8 (2010) 1259–1270.
- [14] Lajarin-Cuesta, R., Nanclares, C., Arranz-Tagarro, J. A., Gonzalez-Lafuente, L., Arribas, R. L., Araujo de Brito, M., Gandia, L., and de Los Rios, C., Gramine Derivatives Targeting Ca(2+) Channels and Ser/Thr Phosphatases: A New Dual Strategy for the Treatment of Neurodegenerative Diseases, *J. Med. Chem.* 59 (2016) 6265–6280.
- [15] Gonzalez, D., Arribas, R. L., Viejo, L., Lajarin-Cuesta, R., and de Los Rios, C., Substituent effect of N-benzylated gramine derivatives that prevent the PP2A inhibition and dissipate the neuronal Ca(2+) overload, as a multitarget strategy for the treatment of Alzheimer's disease, *Bioorg. Med. Chem.* 26 (2018) 2551–2560.
- [16] Scheltens, P., Blennow, K., Breteler, M. M., de Strooper, B., Frisoni, G. B., Salloway, S., and Van der Flier, W. M., Alzheimer's disease, *Lancet* 388 (2016) 505–517.

- [17] Berridge, M. J., Calcium hypothesis of Alzheimer's disease, *Pflugers Arch.* 459 (2010) 441–449.
- [18] Berridge, M. J., Calcium regulation of neural rhythms, memory and Alzheimer's disease, *J. Physiol.* 592 (2014) 281–293.
- [19] Alam, S., Lingenfelter, K. S., Bender, A. M., and Lindsley, C. W., Classics in Chemical Neuroscience: Memantine, *ACS Chem. Neurosci.* 8 (2017) 1823–1829.
- [20] de los Rios, C., Cholinesterase inhibitors: a patent review (2007 – 2011), *Expert Opin. Ther. Pat.* 22 (2012) 853–869.
- [21] Iqbal, K., Liu, F., and Gong, C. X., Tau and neurodegenerative disease: the story so far, *Nat. Rev. Neurol.* 12 (2016) 15–27.
- [22] Rapoport, M., Dawson, H. N., Binder, L. I., Vitek, M. P., and Ferreira, A., Tau is essential to beta -amyloid-induced neurotoxicity, *Proc. Natl. Acad. Sci. U S A* 99 (2002) 6364–6369.
- [23] Medina, M., and Avila, J., The role of extracellular Tau in the spreading of neurofibrillary pathology, *Front. Cell. Neurosci.* 8 (2014) 113.
- [24] Medina, M., and Avila, J., Further understanding of tau phosphorylation: implications for therapy, *Expert Rev. Neurother.* 15 (2015) 115–122.
- [25] Editorial, Alzheimer's disease: expedition into the unknown, *Lancet* 388 (2016) 2713.
- [26] Mullard, A., Sting of Alzheimer's failures offset by upcoming prevention trials, *Nat. Rev. Drug Discov.* 11 (2012) 657–660.
- [27] Gauthier, S., Feldman, H. H., Schneider, L. S., Wilcock, G. K., Frisoni, G. B., Hardlund, J. H., Moebius, H. J., Bentham, P., Kook, K. A., Wischik, D. J., Schelter, B. O., Davis, C. S., Staff, R. T., Bracoud, L., Shamsi, K., Storey, J.

- M., Harrington, C. R., and Wischik, C. M., Efficacy and safety of tau-aggregation inhibitor therapy in patients with mild or moderate Alzheimer's disease: a randomised, controlled, double-blind, parallel-arm, phase 3 trial, *Lancet* 388 (2016) 2873–2884.
- [28] Liu, F., Grundke-Iqbal, I., Iqbal, K., and Gong, C. X., Contributions of protein phosphatases PP1, PP2A, PP2B and PP5 to the regulation of tau phosphorylation, *Eur. J. Neurosci.* 22 (2005) 1942–1950.
- [29] Lajarin-Cuesta, R., Arribas, R. L., and De Los Rios, C., Ligands for Ser/Thr phosphoprotein phosphatases: a patent review (2005–2015), *Expert Opin. Ther. Pat.* 26 (2016) 389–407.
- [30] Zhang, M., Yogesha, S. D., Mayfield, J. E., Gill, G. N., and Zhang, Y., Viewing serine/threonine protein phosphatases through the eyes of drug designers, *FEBS J.* 280 (2013) 4739–4760.
- [31] Sontag, J. M., and Sontag, E., Protein phosphatase 2A dysfunction in Alzheimer's disease, *Front. Mol. Neurosci.* 7 (2014) 16.
- [32] Park, H. J., Lee, K. W., Park, E. S., Oh, S., Yan, R., Zhang, J., Beach, T. G., Adler, C. H., Voronkov, M., Braithwaite, S. P., Stock, J. B., and Mouradian, M. M., Dysregulation of protein phosphatase 2A in parkinson disease and dementia with lewy bodies, *Ann. Clin. Transl. Neurol.* 3 (2016) 769–780.
- [33] Wang, X., Blanchard, J., Grundke-Iqbal, I., Wegiel, J., Deng, H. X., Siddique, T., and Iqbal, K., Alzheimer disease and amyotrophic lateral sclerosis: an etiopathogenic connection, *Acta Neuropathol.* 127 (2014) 243–256.
- [34] Arif, M., Kazim, S. F., Grundke-Iqbal, I., Garruto, R. M., and Iqbal, K., Tau pathology involves protein phosphatase 2A in parkinsonism-dementia of Guam, *Proc. Natl. Acad. Sci. U S A* 111 (2014) 1144–1149.

- [35] Voronkov, M., Braithwaite, S. P., and Stock, J. B., Phosphoprotein phosphatase 2A: a novel druggable target for Alzheimer's disease, *Future Med. Chem.* 3 (2011) 821–833.
- [36] Lipinski, C. A., Lombardo, F., Dominy, B. W., and Feeney, P. J., Experimental and computational approaches to estimate solubility and permeability in drug discovery and development settings, *Adv. Drug Deliv. Rev.* 46 (2001) 3–26.
- [37] Rankovic, Z., CNS Physicochemical Property Space Shaped by a Diverse Set of Molecules with Experimentally Determined Exposure in the Mouse Brain, *J. Med. Chem.* 60 (2017) 5943–5954.
- [38] Wang, J., Zhu, H. T., Chen, S., Xia, Y., Jin, D. P., Qiu, Y. F., Li, Y. X., and Liang, Y. M., Electrophilic Cyclization of Aryl Propargylic Alcohols: Synthesis of Dihalogenated 6,9-Dihydropyrido[1,2-a]indoles via a Cascade Iodocyclization, *J. Org. Chem.* 81 (2016) 10975–10986.
- [39] Hong, X., Tan, Q., Liu, B., and Xu, B., Isocyanide-Induced Activation of Copper Sulfate: Direct Access to Functionalized Heteroarene Sulfonic Esters, *Angew. Chem. Int. Ed. Engl.* 56 (2017) 3961–3965.
- [40] Yu, L., Li, P., and Wang, L., Copper-promoted decarboxylative direct C3-acylation of N-substituted indoles with alpha-oxocarboxylic acids, *Chem. Commun. (Camb)* 49 (2013) 2368–2370.
- [41] Garcia-Frutos, E. M., and Gomez-Lor, B., Synthesis and self-association properties of functionalized C3-symmetric hexakis(p-substituted-phenylethynyl)triindoles, *J. Am. Chem. Soc.* 130 (2008) 9173–9177.
- [42] Wu, P. W., Hsieh, W. T., Cheng, Y. M., Wei, C. Y., and Chou, P. T., Synthesis of 7-azaserotonin: its photophysical properties associated with excited state proton transfer reaction, *J. Am. Chem. Soc.* 128 (2006) 14426–14427.

- [43] Go, M. L., Leow, J. L., Gorla, S. K., Schuller, A. P., Wang, M., and Casey, P. J., Amino derivatives of indole as potent inhibitors of isoprenylcysteine carboxyl methyltransferase, *J. Med. Chem.* 53 (2010) 6838–6850.
- [44] Medina, M., Avila, J., and Villanueva, N., Use of okadaic acid to identify relevant phosphopeptides in pathology: a focus on neurodegeneration, *Mar. Drugs* 11 (2013) 1656–1668.
- [45] Sun, L., Liu, S. Y., Zhou, X. W., Wang, X. C., Liu, R., Wang, Q., and Wang, J. Z., Inhibition of protein phosphatase 2A- and protein phosphatase 1-induced tau hyperphosphorylation and impairment of spatial memory retention in rats, *Neurosci.* 118 (2003) 1175–1182.
- [46] McAvoy, T., and Nairn, A. C., Serine/threonine protein phosphatase assays, *Curr. Protoc. Mol. Biol.* Chapter 18 (2010) Unit18, 18.
- [47] Kalev, P., and Sablina, A. A., Protein phosphatase 2A as a potential target for anticancer therapy, *Anticancer Agents Med. Chem.* 11 (2011) 38–46.
- [48] Augustinack, J. C., Schneider, A., Mandelkow, E. M., and Hyman, B. T., Specific tau phosphorylation sites correlate with severity of neuronal cytopathology in Alzheimer's disease, *Acta Neuropathol.* 103 (2002) 26–35.
- [49] Xing, Y., Xu, Y., Chen, Y., Jeffrey, P. D., Chao, Y., Lin, Z., Li, Z., Strack, S., Stock, J. B., and Shi, Y., Structure of protein phosphatase 2A core enzyme bound to tumor-inducing toxins, *Cell* 127 (2006) 341–353.
- [50] Nimmrich, V., and Eckert, A., Calcium channel blockers and dementia, *Br. J. Pharmacol.* 169 (2013) 1203–1210.
- [51] Reeve, H. L., Vaughan, P. F., and Peers, C., Calcium channel currents in undifferentiated human neuroblastoma (SH-SY5Y) cells: actions and possible

- interactions of dihydropyridines and omega-conotoxin, *Eur. J. Neurosci.* 6 (1994) 943–952.
- [52] Denizot, F., and Lang, R., Rapid colorimetric assay for cell growth and survival. Modifications to the tetrazolium dye procedure giving improved sensitivity and reliability, *J. Immunol. Methods* 89 (1986) 271–277.
- [53] Egea, J., Rosa, A. O., Cuadrado, A., Garcia, A. G., and Lopez, M. G., Nicotinic receptor activation by epibatidine induces heme oxygenase-1 and protects chromaffin cells against oxidative stress, *J. Neurochem.* 102 (2007) 1842–1852.
- [54] Jin Jung, K., Hyun Kim, D., Kyeong Lee, E., Woo Song, C., Pal Yu, B., and Young Chung, H., Oxidative stress induces inactivation of protein phosphatase 2A, promoting proinflammatory NF-kappaB in aged rat kidney, *Free Radic. Biol. Med.* 61 (2013) 206–217.
- [55] Mattson, M. P., Cheng, B., Davis, D., Bryant, K., Lieberburg, I., and Rydel, R. E., beta-Amyloid peptides destabilize calcium homeostasis and render human cortical neurons vulnerable to excitotoxicity, *J. Neurosci.* 12 (1992) 376–389.
- [56] Ueda, K., Shinohara, S., Yagami, T., Asakura, K., and Kawasaki, K., Amyloid beta protein potentiates Ca²⁺ influx through L-type voltage-sensitive Ca²⁺ channels: a possible involvement of free radicals, *J. Neurochem.* 68 (1997) 265–271.
- [57] Arribas, R. L., Romero, A., Egea, J., and de los Ríos, C., Modulation of serine/threonine phosphatases by melatonin: therapeutic approaches in neurodegenerative diseases, *Br. J. Pharmacol.* (2018) DOI: 10.1111/bph.14365.

- [58] Romero, A., Egea, J., Garcia, A. G., and Lopez, M. G., Synergistic neuroprotective effect of combined low concentrations of galantamine and melatonin against oxidative stress in SH-SY5Y neuroblastoma cells, *J. Pineal Res.* 49 (2010) 141–148.
- [59] Groschner, K., Schuhmann, K., Mieskes, G., Baumgartner, W., and Romanin, C., A type 2A phosphatase-sensitive phosphorylation site controls modal gating of L-type Ca^{2+} channels in human vascular smooth-muscle cells, *Biochem. J.* 318 (Pt 2) (1996) 513–517.
- [60] Yu, L., Xu, J., Minobe, E., Kameyama, A., Yang, L., Feng, R., Hao, L., and Kameyama, M., Role of protein phosphatases in the run down of guinea pig cardiac Cav1.2 Ca^{2+} channels, *Am. J. Physiol. Cell Physiol.* 310 (2016) C773–779.
- [61] Li, L., Sengupta, A., Haque, N., Grundke-Iqbal, I., and Iqbal, K., Memantine inhibits and reverses the Alzheimer type abnormal hyperphosphorylation of tau and associated neurodegeneration, *FEBS Lett.* 566 (2004) 261–269.
- [62] Rosini, M., Simoni, E., Caporaso, R., and Minarini, A., Multitarget strategies in Alzheimer's disease: benefits and challenges on the road to therapeutics, *Future Med. Chem.* 8 (2016) 697–711.
- [63] Prati, F., Cavalli, A., and Bolognesi, M. L., Navigating the Chemical Space of Multitarget-Directed Ligands: From Hybrids to Fragments in Alzheimer's Disease, *Molecules* 21 (2016) 466.
- [64] Cai, P., Fang, S. Q., Yang, X. L., Wu, J. J., Liu, Q. H., Hong, H., Wang, X. B., and Kong, L. Y., Rational Design and Multibiological Profiling of Novel Donepezil-Trolox Hybrids against Alzheimer's Disease, with Cholinergic,

- Antioxidant, Neuroprotective, and Cognition Enhancing Properties, *ACS Chem. Neurosci.* 8 (2017) 2496–2511.
- [65] Jameel, E., Meena, P., Maqbool, M., Kumar, J., Ahmed, W., Mumtazuddin, S., Tiwari, M., Hoda, N., and Jayaram, B., Rational design, synthesis and biological screening of triazine-triazolopyrimidine hybrids as multitarget anti-Alzheimer agents, *Eur. J. Med. Chem.* 136 (2017) 36–51.
- [66] Bachurin, S. O., Shevtsova, E. F., Makhaeva, G. F., Grigoriev, V. V., Boltneva, N. P., Kovaleva, N. V., Lushchekina, S. V., Shevtsov, P. N., Neganova, M. E., Redkozubova, O. M., Bovina, E. V., Gabrelyan, A. V., Fisenko, V. P., Sokolov, V. B., Aksinenko, A. Y., Echeverria, V., Barreto, G. E., and Aliev, G., Novel conjugates of aminoadamantanes with carbazole derivatives as potential multitarget agents for AD treatment, *Sci. Rep.* 7 (2017) 45627.
- [67] Shaik, J. B., Palaka, B. K., Penumala, M., Eadlapalli, S., Darla Mark, M., Ampasala, D. R., Vadde, R., and Amooru Gangaiah, D., Synthesis, Biological Evaluation, and Molecular Docking of 8-imino-2-oxo-2H,8H-pyrano[2,3-f]chromene Analogs: New Dual AChE Inhibitors as Potential Drugs for the Treatment of Alzheimer's Disease, *Chem. Biol. Drug Des.* 88 (2016) 43–53.
- [68] Jerabek, J., Uliassi, E., Guidotti, L., Korabecny, J., Soukup, O., Sepsova, V., Hrabínova, M., Kuca, K., Bartolini, M., Pena-Altamira, L. E., Petralla, S., Monti, B., Roberti, M., and Bolognesi, M. L., Tacrine-resveratrol fused hybrids as multi-target-directed ligands against Alzheimer's disease, *Eur. J. Med. Chem.* 127 (2017) 250–262.
- [69] Dgachi, Y., Ismaili, L., Knez, D., Bencheikroun, M., Martin, H., Szalaj, N., Wehle, S., Bautista-Aguilera, O. M., Luzet, V., Bonnet, A., Malawska, B.,

- Gobec, S., Chioua, M., Decker, M., Chabchoub, F., and Marco-Contelles, J., Synthesis and Biological Assessment of Racemic Benzochromenopyrimidinimines as Antioxidant, Cholinesterase, and Abeta1-42 Aggregation Inhibitors for Alzheimer's Disease Therapy, *ChemMedChem* 11 (2016) 1318–1327.
- [70] Cornec, A. S., Monti, L., Kovalevich, J., Makani, V., James, M. J., Vijayendran, K. G., Oukoloff, K., Yao, Y., Lee, V. M., Trojanowski, J. Q., Smith, A. B., 3rd, Brunden, K. R., and Ballatore, C., Multitargeted Imidazoles: Potential Therapeutic Leads for Alzheimer's and Other Neurodegenerative Diseases, *J. Med. Chem.* 60 (2017) 5120–5145.
- [71] Alonso, E., Vieira, A. C., Rodriguez, I., Alvarino, R., Gegunde, S., Fuwa, H., Suga, Y., Sasaki, M., Alfonso, A., Cifuentes, J. M., and Botana, L. M., Tetracyclic Truncated Analogue of the Marine Toxin Gambierol Modifies NMDA, Tau, and Amyloid beta Expression in Mice Brains: Implications in AD Pathology, *ACS Chem. Neurosci.* 8 (2017) 1358–1367.
- [72] Kang, S., Cooper, G., Dunne, S. F., Luan, C. H., Surmeier, D. J., and Silverman, R. B., Structure-activity relationship of N,N'-disubstituted pyrimidinetriones as Ca(V)1.3 calcium channel-selective antagonists for Parkinson's disease, *J. Med. Chem.* 56 (2013) 4786–4797.
- [73] Koh, P. O., Melatonin attenuates decrease of protein phosphatase 2A subunit B in ischemic brain injury, *J. Pineal Res.* 52 (2012) 57–61.
- [74] Gurkoff, G., Shahlaie, K., Lyeth, B., and Berman, R., Voltage-gated calcium channel antagonists and traumatic brain injury, *Pharmaceuticals (Basel)* 6 (2013) 788–812.

- [75] Tan, X. L., Wright, D. K., Liu, S., Hovens, C., O'Brien, T. J., and Shultz, S. R., Sodium selenate, a protein phosphatase 2A activator, mitigates hyperphosphorylated tau and improves repeated mild traumatic brain injury outcomes, *Neuropharmacol.* 108 (2016) 382–393.
- [76] Wang, Y., Lei, Y., Fang, L., Mu, Y., Wu, J., and Zhang, X., Roles of phosphatase 2A in nociceptive signal processing, *Mol. Pain* 9 (2013) 46.
- [77] Zamponi, G. W., Targeting voltage-gated calcium channels in neurological and psychiatric diseases, *Nat. Rev. Drug Discov.* 15 (2016) 19–34.
- [78] Na, Y. M., Le Borgne, M., Pagniez, F., Le Baut, G., and Le Pape, P., Synthesis and antifungal activity of new 1-halogenobenzyl-3-imidazolylmethylindole derivatives, *Eur. J. Med. Chem.* 38 (2003) 75–87.
- [79] Perez, E. G., Ocampo, C., Feuerbach, D., Lopez, J. J., Morelo, G. L., Tapia, R. A., and Arias, H. R., Novel 1-(1-benzyl-1H-indol-3-yl)-N,N,N-trimethylmethanaminium iodides are competitive antagonists for the human $\alpha 4\beta 2$ and $\alpha 7$ nicotinic acetylcholine receptors, *MedChemComm* 4 (2013) 1166–1170.
- [80] Baehn, S., Imm, S., Mevius, K., Neubert, L., Tillack, A., Williams, J. M. J., and Beller, M., Selective ruthenium-catalyzed N-alkylation of indoles by using alcohols, *Chem. - Eur. J.* 16 (2010) 3590–3593, S3590/3591–S3590/3514.
- [81] Bassaco, M. M., Fortes, M. P., Back, D. F., Kaufman, T. S., and Silveira, C. C., An eco-friendly synthesis of novel 3,5-disubstituted-1,2-isoxazoles in PEG-400, employing the Et₃N-promoted hydroamination of symmetric and unsymmetric 1,3-diyne-indole derivatives, *RSC Adv.* 4 (2014) 60785–60797.
- [82] Evans, D. A., Scheidt, K. A., Fandrick, K. R., Lam, H. W., and Wu, J., Enantioselective indole Friedel–Crafts alkylations catalyzed by

- bis(oxazolinyl)pyridine-scandium(III) triflate complexes, *J. Am. Chem. Soc.* 125 (2003) 10780–10781.
- [83] Laha, J. K., Bhimpuria, R. A., Prajapati, D. V., Dayal, N., and Sharma, S., Palladium-catalyzed regioselective C-2 arylation of 7-azaindoles, indoles, and pyrroles with arenes, *Chem. Comm.* 52 (2016) 4329–4332.
- [84] Miranda, S., Lopez-Alvarado, P., Avendano, C., and Menendez, J. C., Convenient synthesis of highly functionalized, 3,4-disubstituted indole building blocks, *Open Org. Chem. J.* 1 (2007) 1–12.
- [85] Sharifi, A., Mirzaei, M., and Naimi-Jamal, M. R., Solvent-free aminoalkylation of phenols and indoles assisted by microwave irradiation, *Monatsh. Chem.* 132 (2001) 875–880.
- [86] Thomsen, R., and Christensen, M. H., MolDock: a new technique for high-accuracy molecular docking, *J. Med. Chem.* 49 (2006) 3315–3321.
- [87] Martinez-Sanz, F. J., Lajarin-Cuesta, R., Gonzalez-Lafuente, L., Moreno-Ortega, A. J., Punzon, E., Cano-Abad, M. F., and de Los Rios, C., Neuroprotective profile of pyridothiazepines with blocking activity of the mitochondrial Na(+)/Ca(2+) exchanger, *Eur. J. Med. Chem.* 109 (2016) 114–123.
- [88] Moro, M. A., Lopez, M. G., Gandia, L., Michelena, P., and Garcia, A. G., Separation and culture of living adrenaline- and noradrenaline-containing cells from bovine adrenal medullae, *Anal. Biochem.* 185 (1990) 243–248.
- [89] Hamill, O. P., Marty, A., Neher, E., Sakmann, B., and Sigworth, F. J., Improved patch-clamp techniques for high-resolution current recording from cells and cell-free membrane patches, *Pflugers Arch.* 391 (1981) 85–100.